Annu. Rev. Earth Planet. Sci. 1999. 27:231–85

THERMOHALINE CIRCULATION: High-Latitude Phenomena and the Difference Between the Pacific and Atlantic

A. J. Weaver, C. M. Bitz, A. F. Fanning, and M. M. Holland
School of Earth & Ocean Sciences, University of Victoria, P.O. Box 3055, Victoria, British Columbia, Canada V8W 3P6; e-mail: weaver@uvic.ca

KEY WORDS: thermohaline circulation, climate variability, ocean circulation, Arctic Ocean

ABSTRACT

Deepwater formation, the process whereby surface water is actively converted into deep water through heat and freshwater exchange at the air-sea interface, is known to occur in the North Atlantic but not in the North Pacific. As such, the thermohaline circulation is fundamentally different in these two regions. In this review we provide a description of this circulation and outline a number of reasons as to why deep water is formed in the North Atlantic but not in the North Pacific. Special emphasis is given to the role of interactions with the Arctic Ocean. We extend our analysis to discuss the observational evidence and current theories for decadal-interdecadal climate variability in each region, with particular focus on the role of the ocean. Differences between the North Atlantic and North Pacific are highlighted.

INTRODUCTION

The discovery by Ellis (1751), captain of the ship *Earl of Halifax*, that the deep water at 25′13″N, 25′12″W was cold appears almost trivial to us today. In fact, the realization that deep water is cold even in equatorial regions has profound implications. The analysis of water mass properties has traced the cold deep water back to its polar origin. Since the surface-intensified, wind-driven gyres are not generally thought capable of driving the deep meridional flows

0084-6597/99/0515-0231$08.00

required for such excursions, the quest for the deep circulation leads directly to the thermohaline circulation.

In his remarkable essay, Thompson, Count Rumford (1798) (Figure 1), was the first to envision a meridional overturning driven by cooling at high latitudes and warming at the equator. Thompson (1798) pointed out that surface waters that were cooled at high latitudes must sink and spread out equatorward and noted the surface and deep ocean temperature observations of Ellis (1751) and Kirwan (1787) as "incontrovertible proof of the existence of currents of cold water at the bottom of the sea." He further argued that the Gulf Stream in the North Atlantic was the surface manifestation of this thermally driven meridional overturning.

In this same essay, Thompson, Count Rumford (1798), discussed the concept of thermal stability of the oceans and noted the moderating effect the oceans had on climate. He wrote:

> The vast extent of the ocean, and its great depth, but still more numerous its currents, and the power of water to absorb a vast quantity of Heat, render it peculiarly well adapted to serve as an equalizer of Heat.

He further wrote:

> There is, however, a circumstance by which these rapid advances of winter are in some measure moderated. The earth, but more especially the *water*, having imbibed a vast quantity of Heat during the long summer days, while they receive the influence of the sun's vivifying beams; this Heat, being given off to the cold air which rushes in from polar regions, serves to warm it and soften it, and consequently to diminish the impetuosity of its motion, and take off the keenness of its blast.

These remarkable and colorful insights into the large-scale interaction between the oceans and the atmosphere, the formation of deep waters, and the moderating effect that the oceans have on climate have largely stood unchanged for two centuries.

THE THERMOHALINE CIRCULATION IN THE NORTH ATLANTIC AND PACIFIC OCEANS

The ocean is well known to have a moderating effect on climate through several mechanisms. It is the buffer that moderates daily, seasonal, and even interannual temperature fluctuations. Comparison of the maritime climate of Victoria, British Columbia (48°25′N, 123°22′W, Figure 2, with average temperatures of 4°C in January and 16°C in July), with the continental climate of Winnipeg, Manitoba (49°54′N, 97°14′W, with average temperature of −18°C in January and 20°C in July), shows the moderating effect of the ocean. The ocean also acts as a large-scale conveyor that transports heat from low to high latitudes,

Figure 1 Portrait of Sir Benjamin Thompson, Count Rumford, taken in 1798 at the age of 45 (taken from Ellis 1868).

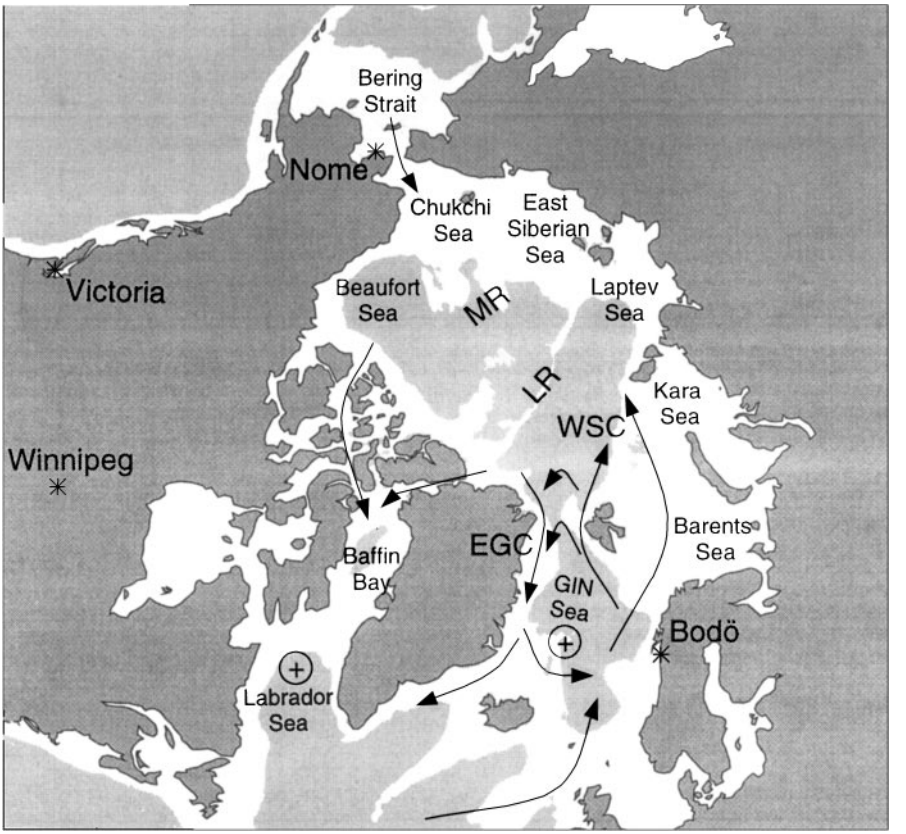

Figure 2 The major oceanic exchanges between the Arctic and the high-latitude oceans including the East Greenland Current (EGC) and the West Spitsbergen Current (WSC). Depths greater than 1000 m are shaded, and the Mendeleyev (MR) and Lomonosov (LR) ridges, as well as the general sites of deepwater formation (*circled pluses*), are also illustrated. Also shown are the locations of Victoria, British Columbia; Winnipeg, Manitoba; Bodö, Norway; Nome, Alaska.

reducing latitudinal gradients of temperature. Much of the oceanic heat transport is thought to be associated with the thermohaline circulation (that part of the ocean's circulation that is driven by fluxes of heat and fresh water through the ocean's surface). In the North Atlantic, intense heat loss to the overlying atmosphere causes deep water to be formed in the Greenland, Iceland, and Norwegian (GIN) Seas (Figure 2). These sinking regions are fed by warm, saline waters brought by the thermohaline circulation from lower latitudes. No such deep sinking exists in the Pacific. Again, if one compares the climates of

Bodö, Norway (67°17′N, 14°25′E, Figure 2, with average January temperature of −2°C and average July temperature of 14°C), to that of Nome, Alaska (64°30′N, 165°26′W, with average January temperature of −15°C and average July temperature of 10°C) (both of which are at similar latitudes and on the western flanks of continental land masses), one directly sees the impact of the poleward heat transport of the thermohaline circulation. The ocean can also regulate climate through its ability to store both anthropogenic and natural greenhouse gases.

The now classical picture of the overturning in a meridional plane driven by the poleward decrease in the net surface radiation is shown in Figure 3, taken from Wyrtki (1961). Warm, light water flows poleward at the surface and loses its buoyancy by intense cooling at high latitudes. The newly formed deep water spreads equatorward and diffuses slowly upward through the thermocline, at a rate of only a few meters per year (Bretherton 1982). With the additional constraint of geostrophy (the balance between horizontal pressure gradient and Coriolis forces), such a meridional flow must be supported by either an east-west pressure gradient, for which lateral boundaries are required, or friction, as in the circumpolar ocean—e.g. the analytic model of Wyrtki (1961).

The approach initiated by Stommel (1957) and pursued by Stommel & Arons (1960) was to isolate the deep ocean by a level surface at some depth upon which the vertical velocity was everywhere specified. The flow was supposed

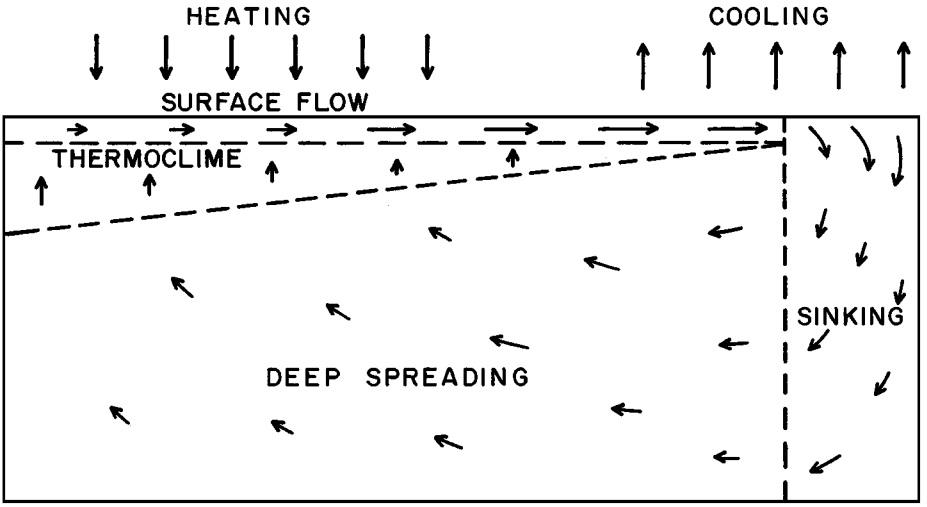

Figure 3 The now classical model of a purely thermohaline circulation driven by heating at low latitudes and cooling at high latitudes (redrawn from Wyrtki 1961).

independent of depth in the deep layer and so was dictated by the divergence/convergence needed to supply the vertical mass transport across the level of no motion. As the true distribution of the vertical velocity in the world ocean is poorly known (although Gordon 1986, Broecker 1991, and Schmitz & McCartney 1993 refer to the circumpolar ocean as the primary site for the upwelling), the assumption of uniform upwelling was made, except for specified high-latitude deep sinking regions. In the interior the geostrophic balance was expressed through the Sverdrup relation:

$$\beta v = f w_z \tag{1}$$

where v is the northward velocity and f is the Coriolis parameter with meridional gradient β. In a flat-bottomed ocean of depth H, with the vertical velocity $w = 0$ at a depth $z = -H$, the vertical integration of Equation 1 over the deep layer shows that the vertically integrated deep flow must be poleward. This can be reconciled with the above description since continuity requires that a narrow, rapid, equatorward western boundary current develop to feed the interior flow. In a zonal average the equatorward boundary current dominates the poleward interior flow, and the two-dimensional overturning cell described by Wyrtki (1961) is recreated.

Figure 4 is a sketch of an idealized deep ocean circulation as obtained using the Stommel-Arons approach. In this example, two sources of deep sinking are prescribed: one in the northern North Atlantic and one in the Southern Ocean, in approximate agreement with the observed deep circulation today. The three main oceans are represented by flat-bottomed basins bounded by parallels and meridians. The geostrophic flow in the interior is then poleward in both hemispheres, but cross-equatorial transport is possible in the western boundary currents if the strength of the deepwater source in a hemisphere is not precisely balanced by the uniform upwelling over the rest of the hemisphere.

Kawase (1987) refined the Stommel-Arons model by parameterizing (rather than prescribing) the cross-interfacial flow as proportional to the interfacial displacement. In his baroclinic (inverted reduced gravity) model, the vertical velocity then acts as a damping term in the continuity equation. When the damping is strong, the westward radiation of Rossby waves into the interior is impeded, and the deep flow is confined to boundary layers along the coasts and the equator. For weak damping, the normal Stommel-Arons circulation is duplicated.

To obtain a first idea of the importance of wind in the deep ocean, Wyrtki (1961) considered the distribution of Ekman pumping and Ekman suction at the base of the surface layer in the Southern Hemisphere. He imagined four ocean layers outcropping at successively higher latitudes and bounded by the limits of the zones of wind-driven convergence and divergence. The four layers were compared to the observed stratification of the ocean, with thermocline water

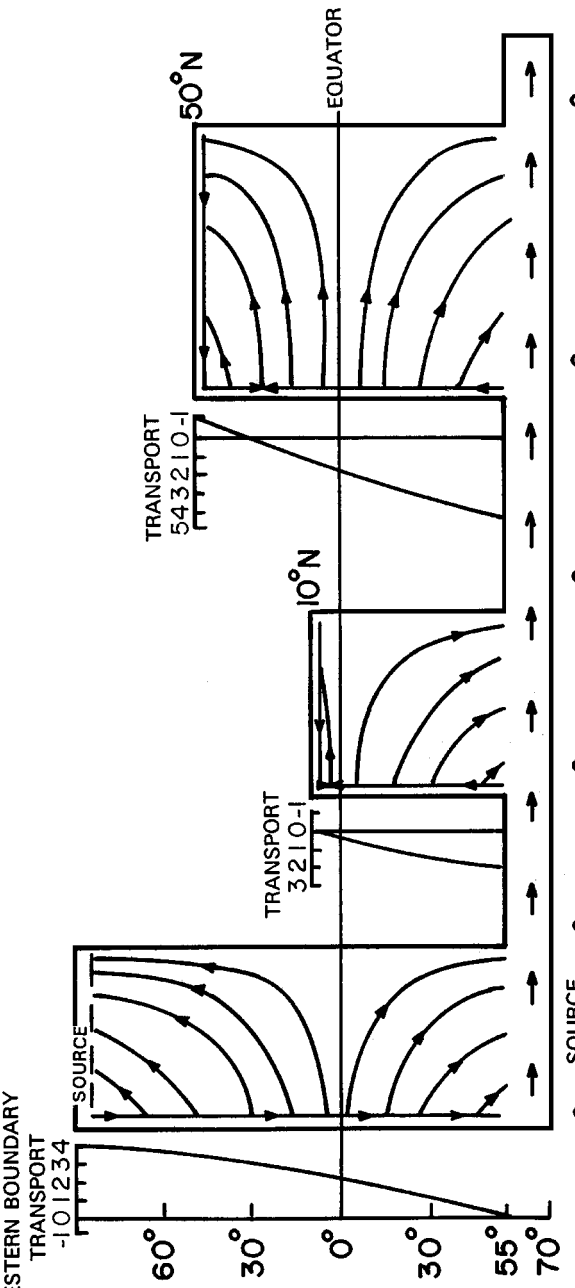

Figure 4 The Stommel-Arons model of the deep ocean thermohaline circulation with two point sources and uniform upwelling (redrawn from Warren 1981, after Kuo & Veronis 1973).

lying above intermediate water, deep water, and bottom water. In his analytic model the wind-induced meridional transport was calculated to be nonzero even in the lowest layer, although much weaker than in the overlying layers.

A similar partitioning of the sub–mixed-layer ocean into four layers was used by Yin et al (1992) in a numerical model, with the goal of studying the competition between the surface-driven Ekman pumping and the upwelling caused by the deep thermohaline circulation. In their experiments, outcropping was not permitted, but one or more point sources of deep sinking could be prescribed. The density structure was again specified, and cross-isopycnal flow was parameterized in the manner of Kawase (1987). They found that in the absence of deepwater formation the circulation of the deep ocean was several orders of magnitude weaker than that of the upper ocean. The introduction of a deepwater source at high latitudes in the Northern Hemisphere, channeling water from the first model layer into the third, created a pattern of surface convergence and divergence at depth that was superimposed on the wind-driven circulation. This resulted in the enhancement of the poleward western boundary current in the thermocline layer and the appearance of an equatorward undercurrent in the deep layer, in close analogy to the interaction between deepwater formation in the northern North Atlantic and the Gulf Stream (except that the thermodynamic processes causing the deep convection were not modeled). In Yin et al's calculations, the speed of the flow in the deep layer was increased by a factor of about 10 through the imposition of a northern deepwater source of magnitude 20 Sv (1 Sv $= 10^6$ m^3 s^{-1}). When this was supplemented by a bottom-water source in the opposite hemisphere, a northward-flowing western boundary current appeared in the lowest layer, resulting in the type of layered circulation that Stommel & Arons' (1960) original theory was unable to describe. This second source had the additional effect of increasing the cross-interfacial velocities in the model so that the deep water from the north penetrated less far south before detraining completely.

In the Stommel-Arons approach, the meridional gradient of temperature at the surface and the associated secondary circulation (eastward surface flow as demanded by geostrophy, leading to an eastern sea level rise and subsequently setting up an east-west pressure gradient which drives the poleward flow) is presented as less fundamental to the thermohaline circulation than the formation of deep water at high latitudes (corresponding to a sink of mass at the surface and a source at depth). The interior flow is determined by vorticity conservation, and any poleward heat transport is more closely related to the requirement that the circulation be closed by a fast poleward (frictional) western boundary current than to the meridional temperature gradient itself.

Two distinct forms of deepwater formation are recognized: near-continent and open ocean (Killworth 1979). The former involves one of two simple processes: intense evaporation or more typically brine rejection above a continental

shelf produces dense water, which sinks down and along the slope under the combined forces of gravity, friction, and the Coriolis force (Killworth 1983); alternatively, potentially supercooled water may be formed at the base of a thick ice shelf during freezing or melting, and this dense water may in turn flow downslope (Foldvik & Gammelsrød 1988, Grumbine 1991). By contrast, open ocean convection is observed in areas remote from land and is characterized by a large-scale cyclonic mean circulation, which causes a doming of the isopycnals and weakens the static stability over an area tens of kilometers wide. The convection itself is short-lived, is restricted to a narrow circumference, and is typically driven through intense surface cooling. These narrow convective chimneys are almost purely vertical and usually do not entrain large volumes of surrounding water as in near-continent convection (Killworth 1979, 1983).

Both types of deep convection have been observed in the Mediterranean (Killworth 1983, Leaman & Schott 1991), but the dense salty outflow that exits into the Atlantic gains buoyancy by mixing with lighter environmental water and spreads out at middepth rather than sinking to the bottom (Warren 1981, see also Armi & Farmer 1988). Similar saline outflows have been detected issuing at middepth from the Red Sea and Persian Gulf, but each amounts to less than 0.5 Sv in transport (Siedler 1969, Warren 1981). Deep convection occurs at a number of locations around Antarctica, but the dense bottom water is susceptible to being trapped by topographic sills (as in the Bransfield Strait) or by local circulation patterns, not excluding the Antarctic Circumpolar Current (ACC) (Killworth 1983).

Deepwater formation in the Ross Sea has recently been estimated as 13 Sv (Jacobs et al 1985). While Ross Sea deepwater may contribute significantly to Antarctic Bottom Water (AABW) production, it is thought that the major source of AABW (approximately 80 percent) is in the Weddell Sea (Foldvik & Gammelsrød 1988).

In summary, two main bottom-water masses exist whose trajectories can be traced by their temperature and salinity characteristics throughout the rest of the world ocean. These are (*a*) the component of AABW, which is largely produced in the Weddell Sea before mixing with Circumpolar Deep Water in the ACC and then flowing into the major ocean basins; and (*b*) North Atlantic Deep Water (NADW), which lies above the AABW at all latitudes except north of 40°N in the North Atlantic (Mantyla & Reid 1983). The North Pacific, although a source of North Pacific Intermediate Water (NPIW), is not a source of bottom water for reasons to be discussed later.

North Atlantic

The general features of the circulation in the North Atlantic have been well known for many years, although refinements are continually forthcoming. It

is not the purpose of this review to give an exhaustive description of the North Atlantic Ocean circulation, and the reader is referred to the classic works of Ivers (1975), Worthington (1976), and Krauss (1986) for more historical details regarding the refinement of our understanding. More recent reviews are given by Schmitz & McCartney (1993) and Schmitz (1995). In this section we focus primarily on recent developments in our understanding of the thermohaline circulation of the North Atlantic.

The Greenland Sea has long been known to be a major deep-water formation site (Killworth 1979, Warren 1981), and in more recent years, deep convection has actually been observed (Rudels et al 1989, Rhein 1991, Schott et al 1993). Warm, very saline near-surface water from the Atlantic circulates counterclockwise from the Norwegian Sea into the Greenland Sea (Aagaard et al 1985b), where intense winter cooling can induce convection, causing the wintertime properties of the water in the cyclonic gyre to become practically homogeneous in the vertical.

The northern seas are separated from the North Atlantic by the Greenland-Scotland ridge, with a maximum depth of only about 600 to 800 m. Hence the renewal of the deep North Atlantic is actually fed by an overflow of intermediate-depth water from the GIN Seas (Aagaard et al 1985b). About 1 Sv of northern source water passes between Iceland and the Faroe Islands (Meincke 1983) and about 1.7 Sv passes between the Faroe Islands and Scotland (Borenäs & Lundberg 1988, Saunders 1990) (see Figure 5). As these overflow waters flow southwestward in a deep western boundary current, they entrain surrounding waters, yielding 3.2 Sv of transport southeast of Iceland (Saunders 1996). Although it is unclear what happens to the rest of the waters (most likely there is 0.8 Sv of recirculation in the deep Iceland Basin, south of Iceland), a strong constraint on the amount of Iceland-Faroes-Scotland ridge overflow water entering the western Atlantic basin, via transport as a deep boundary current along the Mid-Atlantic Ridge, is provided by recent measurements of 2.4 Sv through the Charlie Gibbs Fracture Zone (Saunders 1994).

In addition, a nearly equal volume (2.9 Sv, Ross 1984) of slightly colder northern source water passes over the shallow sill in the Denmark Strait, rapidly entraining surrounding water (Price & Baringer 1994) to yield about 5.1 (5.2) Sv 160 (320) km downstream from the sill (Dickson & Brown 1994). At 480 km downstream from the sill, Dickson et al (1990) and Dickson & Brown (1994) find 10.7 Sv of deep transport. Dickson & Brown (1994), in reference to McCartney (1992), provide compelling arguments suggesting that the difference between the observed transport (10.7 Sv) and the overflow transport plus Charlie Gibbs Fracture Zone transport (5.1 Sv + 2.4 Sv = 7.5 Sv) is largely caused by entrainment of recirculating cold, relatively fresh Labrador Sea water (see below). Still farther downstream, off the tip of Greenland, Clarke (1984) found 13.3 Sv of deep transport, increased from upstream through

Table 1 Thermohaline transport (in Sv) summary from Schmitz & McCartney (1993)

Water type	32°S	24°N
Thermocline water	8	13
Intermediate water (AAIW)	5	—
Deep water (NADW)	−17	−18
Bottom water (AABW)	4	5

additional recirculating components and water mass entrainment. The deep western boundary undercurrent is thought to be about 200 to 300 km wide and to transport about 13 to 14 Sv of newly formed NADW (Warren 1981, McCartney & Talley 1984, Schmitz & McCartney 1993, Schmitz 1995) southward and eventually to encounter northward flowing AABW. Despite the high salinity of the NADW (further enhanced by mixing with Mediterranean water at midlatitudes), at such great pressures the colder AABW has higher density and passes below the NADW.

Schmitz & McCartney (1993) (see also Lee et al 1996) put forth a consistent picture of the thermohaline circulation (as summarized in Table 1) based on the 32°S transport estimates of Rintoul (1991) and the 24°N estimates of Schmitz & Richardson (1991) and Schmitz et al (1992). These estimates are consistent with those of Hall & Bryden (1982), who estimated 18 Sv, and Roemmich & Wunsch (1985), who estimated 17 Sv of total overturning at 24°N. That is, about 13 Sv of cold, fresh Antarctic Intermediate Water (AAIW) formed in the sub-Antarctic South Pacific and the Scotia Sea flows into the South Atlantic, about 8 Sv of which is converted into thermocline water through mixing by the time it reaches 32°S (Rintoul 1991). Further mixing converts the remaining 5 Sv of AAIW into thermocline water as it approaches the equator (Schmitz & McCartney 1993). At 24°N there is 13 Sv of thermocline water that flows northward into the high northern North Atlantic, where it is converted into NADW. AABW, originating in the Weddell Sea, and to a lesser extent the Ross Sea, flows into the South and North Atlantic, where it is modified into and exported as NADW into the Southern Ocean.

The northward flowing AABW and southward flowing NADW in the western Atlantic are apparently well described by the Stommel-Arons theory. However, the AABW stream deviates from the theory by crossing over to the eastern side of the basin upon reaching the equator, to lie up against the western slope of the Mid-Atlantic Ridge at 8 to 16°N. Warren (1981) offers a topographic explanation for this, whereas Kawase (1987) suggests buoyancy damping of Rossby waves. In either case, by the middle latitudes this flow has diffused laterally enough that it is no longer distinguishable in the form of a boundary current (Warren 1981).

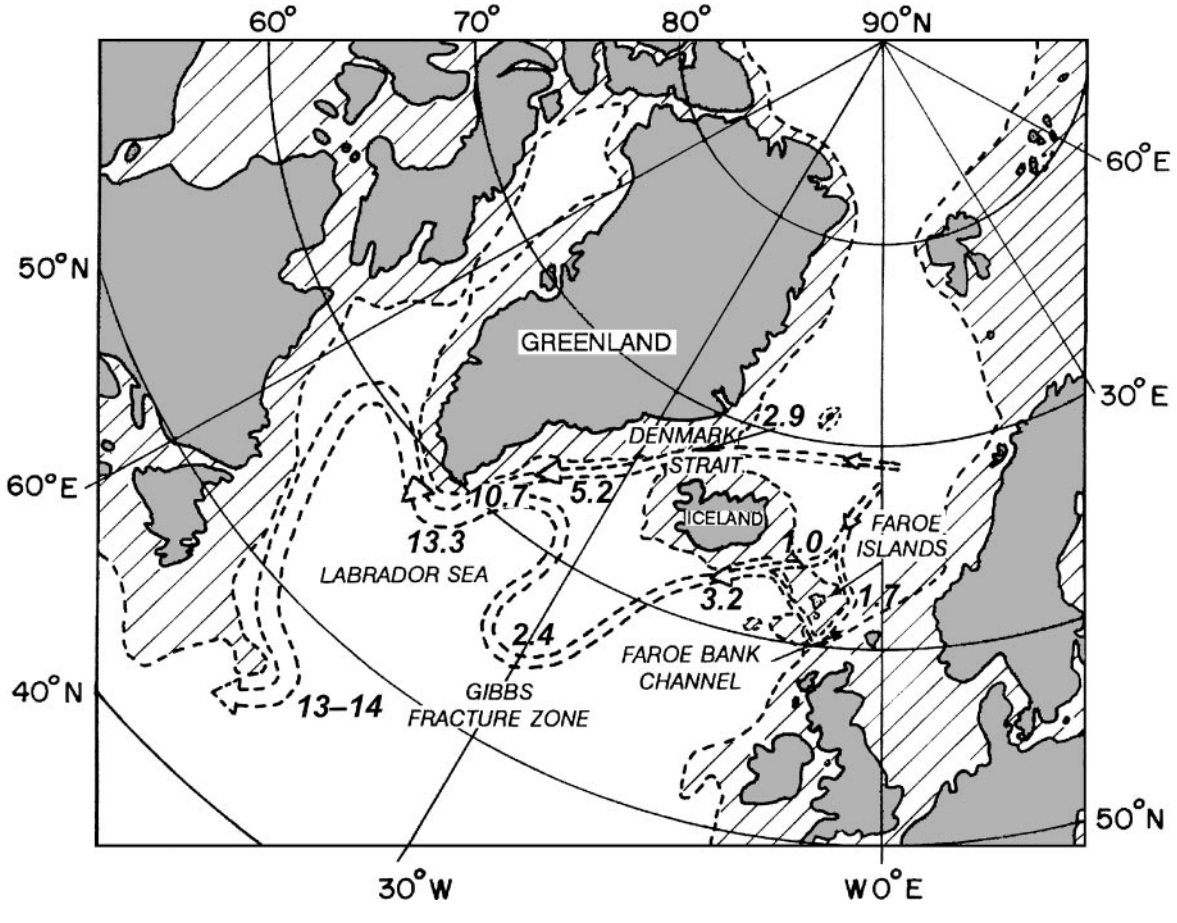

Figure 5 The deep circulation in the northern North Atlantic (redrawn from Warren 1981). The transports (in Sv) at various locations (discussed in the text) are added to the schematic (adapted from Dickson et al 1990 and Dickson & Brown 1994). *Hatched areas* show the continental shelf region.

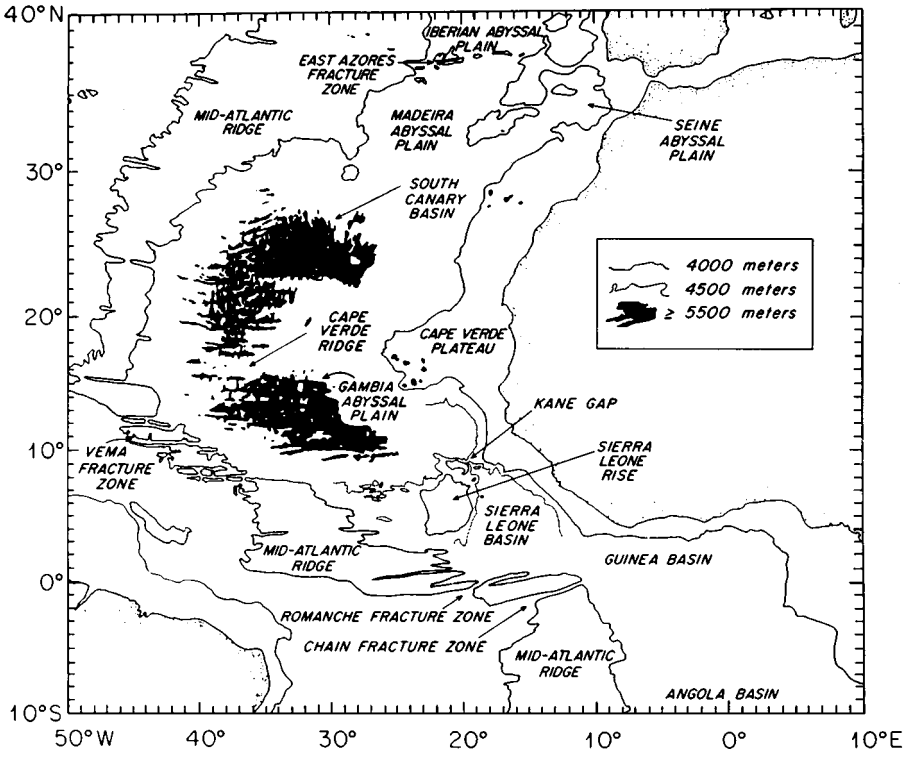

Figure 6 The major topographic features of the eastern North Atlantic (taken from McCartney et al 1991).

The Vema Fracture Zone near 10°N (see Figure 6) is the principal outlet for the deep flow of AABW into the eastern basins of the North Atlantic (Mantyla & Reid 1983, McCartney et al 1991), although farther south, the Romanche Fracture Zone (Figure 6) allows AABW to flow into the deep equatorial and southeastern Atlantic basins (Mantyla & Reid 1983, McCartney et al 1991). In the eastern North Atlantic, the deep water, which has passed through the Vema Fracture Zone, flows both northward and eastward as deep boundary currents trapped against the major topographic features (Figure 6) of the area (McCartney et al 1991).

North Pacific

The deepest connection to the Antarctic in the Pacific sector is toward Drake Passage in the east. The water supplying the central part of the ocean is therefore the lighter water from south of the Campbell Plateau (Figure 7). The

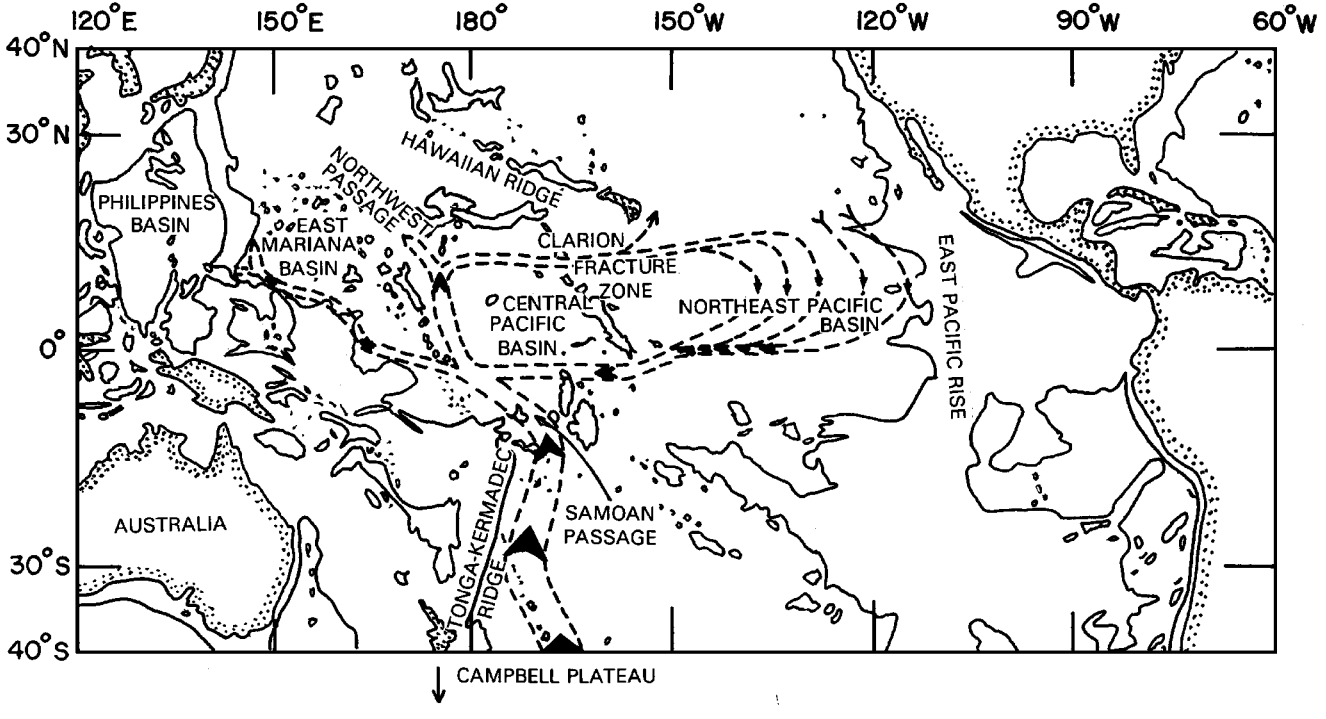

Figure 7 Topographic features of the deep near-equatorial Pacific Ocean as depicted by the 4-km isobath. The schematic representation of the spread of deep Antarctic/circumpolar water is also shown as hypothesized by Johnson (1990) and Johnson & Toole (1993) (redrawn from Johnson 1990 and Johnson & Toole 1993).

effective western boundary for the deep South Pacific is New Zealand and the Tonga-Kermadec Ridge, where a northward boundary current transporting about 19 Sv has been reported (Warren 1973). Above it, there appears to be a weak southward flow whose source is thought to be the North Pacific. Figure 7, taken from Johnson (1990) and Johnson & Toole (1993), is a schematic diagram of the transport of the Antarctic/circumpolar water through the deep basins of the near-equatorial Pacific. About 12 Sv flows northward at 12°S (Taft et al 1991) with about 6 Sv entering the Samoan Passage (Taft et al 1991). The outflow from the Samoan Passage, together with transport of unknown magnitude through gaps in the Robbie Ridge (slightly to the west of the Samoan Passage) and westward recirculated water, feeds deep western boundary currents in the East Mariana and central Pacific Basins, with estimated transports of 5.8 Sv and 8.1 Sv, respectively (Johnson 1990, Johnson & Toole 1993). A relatively weak and broad southward return flow of about 4.7 Sv has also been observed off the western side of the East Pacific Rise in the northeast Pacific Basin (Johnson & Toole 1993).

For many years there was little evidence of deep western boundary currents in the North Pacific (see Johnson 1990 and Hallock & Teague 1996 for reviews), although deep waters clearly had the signature of AABW. Off the Aleutian Islands, however, deep boundary currents were detected (Warren & Owens 1988). Warren (1981) argued that the North Pacific topography was too rough and complex, whereas Joyce et al (1986) argued that the deep flow was too slow for direct observation of deep western boundary currents. Nevertheless, recent observations by Hallock & Teague (1996) (Figure 8) provide compelling evidence for their existence off the east coast of Japan, albeit with a high degree of variability and weak nature. Figure 8, taken from Hallock & Teague (1996), shows a schematic representation of abyssal circulation as proposed by Warren & Owens (1988) and extended by Hallock & Teague (1996). Hallock & Teague (1996) further document the existence of a weak southward flowing deep western boundary current along the slope and inshore of the Japan Trench with a generally northward flow over the trench below the Kuroshio Current (see Figure 8). Their comprehensive review of earlier observations is consistent with the schematic, as are the recent deep geostrophic circulation estimates of Reid (1997).

Although there are no sources of deep water in the North Pacific, intermediate waters, characterized by a salinity minimum in the subtropical gyre at depths of 300 to 800 m within a narrow density range of 26.7 to 26.9σ_θ (Talley 1993), are locally produced.[1] This water mass is mainly constrained to

[1]σ_θ is a measure of the potential density of seawater (ρ_θ): $\sigma_\theta = \rho_\theta - 1000$. Potential density is computed by using potential temperature in the equation of state for seawater. The potential temperature of water is the temperature that water would have if it were adiabatically (no external sources or sinks of heat) brought to the surface of the ocean.

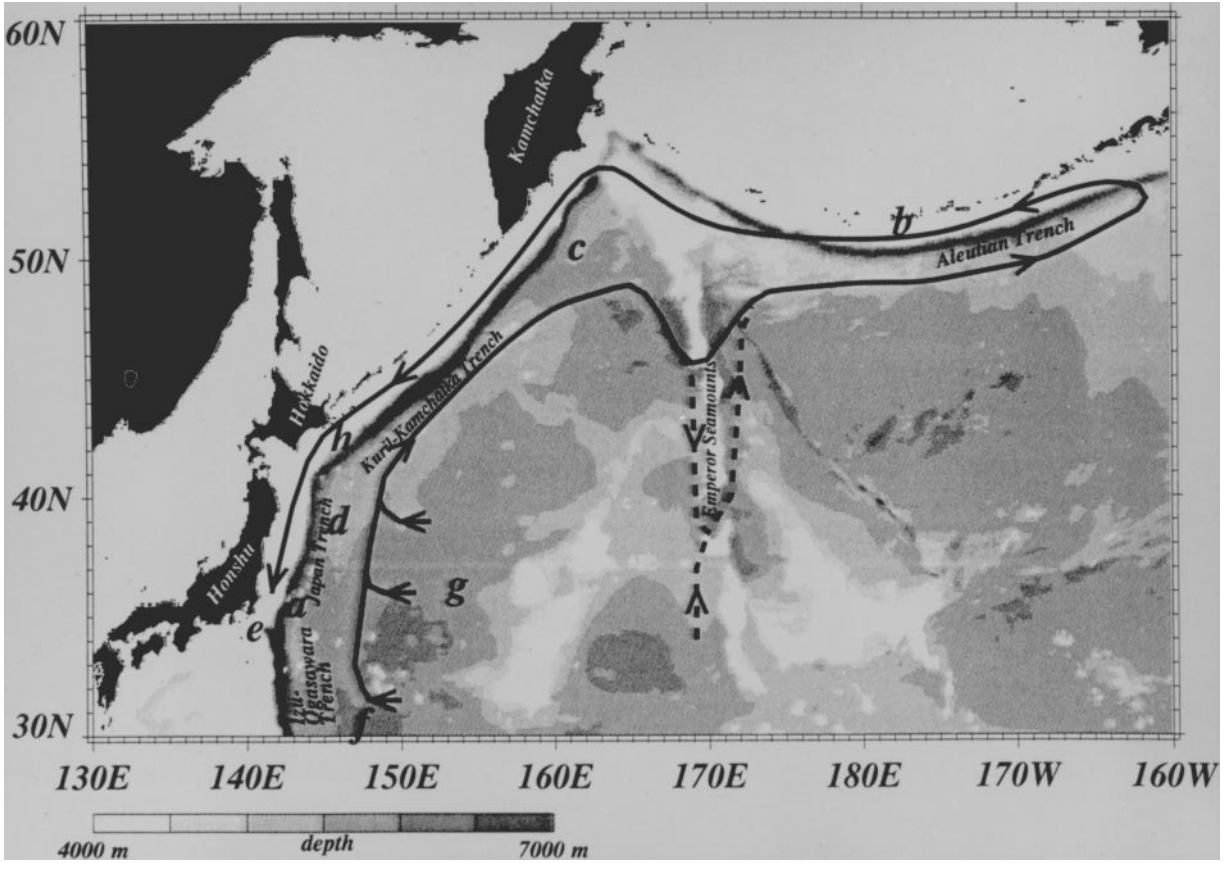

Figure 8 Diagram of the deep circulation in the North Pacific (reproduced from Hallock & Teague 1996) as suggested by Warren & Owens (1988) and modified by Hallock & Teague (1996). The letters indicate references where supporting measurements for this reconstruction are presented (see references in Hallock & Teague 1996).

the subtropical gyre, unlike the Labrador Sea intermediate water mass which is largely confined to the subpolar gyre of the North Atlantic (Talley & McCartney 1982).

Over the past few years, a consistent picture of the formation of North Pacific intermediate water (NPIW) has become apparent. It appears that the original source water for NPIW is sinking in the Sea of Okhotsk (Talley 1991, Yasuda et al 1996, Yasuda 1997, Watanabe & Wakatsuchi 1998). Yasuda (1997) suggests that about 1 Sv of Sea of Okhotsk water (within the 26.6- to 27-σ_θ range) outflows and mixes with warmer and more saline western subarctic gyre water to form Oyashio water. Near the coast, a branch of the Oyashio Current transports newly formed Oyashio water at a rate of about 3 to 7 Sv (Yasuda 1997) past the southern Kuril Islands and Hokkaido before turning eastward in the Kuroshio extension. The distinct signature of NPIW is then formed through mixing in the Kuroshio-Oyashio mixed-water region where the relatively cold, fresh Oyashio waters are overrun by warmer, more saline Kuroshio waters (Hasunuma 1978, Talley 1993, Talley et al 1995, Yasuda et al 1996, Yasuda 1997).

Why Deep Water Forms in the Atlantic but Not in the Pacific

One of the most distinctive characteristics of the present-day global thermohaline circulation is the well-known asymmetry between the Atlantic and Pacific Oceans, with active deep-water formation ongoing in the northern North Atlantic and the oldest water of the world ocean in the deep North Pacific. A central, yet unanswered question concerning the thermohaline circulation is why deep water currently forms in the northern North Atlantic but not in the North Pacific. It is still an open question whether the absence of North Pacific Deep Water (NPDW) is a fundamental aspect of global circulation or a coincidental feature of the present state of the climate. Based on the paleoclimatic record, Keigwin (1987) suggested that even at the Last Glacial Maximum (LGM) (21 KYR), when NADW formation was reduced and shallower than today, NPDW production did not occur. Shackleton et al (1988) also found that during glacial times, deep Pacific water had a ventilation age about 500 years greater than that today, consistent with the results of Keigwin (1987). They further suggested that deep-ocean ventilation rapidly increased around the time of deglaciation, to yield a ventilation age about 500 years less than today. Other paleoclimatic reconstructions for the LGM have suggested the possibility, albeit with large uncertainty, of increased NPIW formation at the LGM (Curry et al 1988, Duplessy et al 1988). Although Berger (1987) suggests that NPDW may have formed during glacial times, he also concedes that increased AABW could also explain his findings. Similarly, Dean et al (1989) provide evidence to support the seasonal formation of a North Pacific deepwater mass during the last glacial-interglacial transition, but they too concede that their results

could be explained by a decreased flux of organic matter during this transition. Ventilation of the deep North Atlantic, in contrast, is thought to have reoccurred throughout the Quaternary, although the intensity may have fluctuated significantly through the glacial-interglacial cycles (Broecker & Denton 1989, Boyle 1990, Oppo & Fairbanks 1990).

It is apparent therefore that proxy indicators have by no means drawn a consistent case for the formation of NPDW during the last glaciation or the transition from it to the present Holocene. Two coupled atmosphere-ocean modeling studies available for the LGM (Ganopolski et al 1998, Weaver et al 1998) are also inconsistent in this regard. In their zonally averaged ocean model coupled to an idealized atmospheric model, Ganopolski et al (1998) find increased NPIW formation at the LGM. On the other hand, using a more realistic ocean general circulation model (GCM) coupled to a simpler atmospheric energy-moisture balance model, Weaver et al (1998) find no change in NPIW rates. Neither of these studies supports the hypothesis that NPDW occurred during the LGM.

Warren (1983) singles out the more stable stratification of the North Pacific (where surface waters are on average 32.8 psu and deep waters are 34.6 to 34.7 psu compared with 34.9 psu and 34.9 to 35.0 psu in the North Atlantic) as the explanation for the present-day occurrence of deepwater formation in the North Atlantic but not in the North Pacific. This follows because even if North Pacific waters are cooled to their freezing point (-1.8°C), they are so fresh that they can sink to a depth of only a few hundred meters (Broecker 1991). Warren (1983) identifies a number of causes for this. For example, there is nearly twice as much evaporation over the North Atlantic as over the North Pacific: 103 cm/yr versus 55 cm/yr averaged over the North Atlantic and Pacific, respectively (Baumgartner & Reichel 1975). The water introduced into the northern North Atlantic from lower latitudes is more saline than its counterpart in the Pacific, and the residence time of this water in the region of net precipitation at high latitudes is shorter. However, as Warren (1983) concedes, none of these factors is truly independent of the already existing thermohaline circulation in the North Atlantic. The salinities of the surface and bottom water masses are similar because the one is being actively converted into the other; the higher evaporation is related to higher sea surface temperatures (SSTs), which are due in part to the greater northward advection of warm subtropical water by the Gulf Stream, but the Gulf Stream itself is partly thermohaline-driven (Holland 1973); and finally, the thermohaline contribution to the western boundary current partly accounts for the faster throughflow rate.

Many geographical clues to the asymmetry of the thermohaline circulation in the two oceans do, of course, exist. The first and most obvious one is that the North Atlantic extends farther north than the North Pacific and has a deeper connection with the Arctic. Schmitt et al (1989) have further suggested that

the narrower width of the Atlantic compared to the Pacific also causes a greater fraction of its area to be susceptible to the incursions of dry cold continental air that favor evaporation and heat loss at the sea surface. In situ measurements of heat transport across 24°N in the Atlantic (Hall & Bryden 1982) and Pacific (Bryden et al 1991) Oceans are 1.2 $\pm$ 0.3 PW (1 PW $= 10^{15}$ W) and 0.76 $\pm$ 0.3 PW, respectively. The larger zonal extent of the Pacific allows for larger east-west temperature contrasts so that gyre heat transport in the horizontal plane may be large enough to offset the need for a component in the meridional plane (Wang et al 1995). Finally, Reid (1961) has hypothesized that the poleward extension of South America compared with south Africa might impede the transport of fresh water out of the Pacific into the Atlantic by the Antarctic Circumpolar Current (ACC).

The sign of the atmospheric water vapor transport between the Atlantic and Pacific (e.g. Broecker et al 1990) is also important evidence, since this has been suggested to be the driving force for the global conveyor belt (Broecker et al 1985, Broecker 1991). The narrow Isthmus of Panama at low latitudes allows the export of water vapor from the Atlantic to the Pacific via the trade winds (Weyl 1968), whereas the Rocky Mountains along the west coast of North America block a similar export from the Pacific by the westerlies at higher latitudes. The result of these differences is that the net Atlantic-to-Pacific atmospheric fresh-water flux in the present climate is thought to be about 0.45 Sv (Baumgartner & Reichel 1975). The circulation of fresh water within the boundaries of the Atlantic alone is equally important to the maintenance of the conveyor belt, since the formation of dense water at high latitudes depends on counteracting the atmospheric transport of water vapor from low to high latitudes (Broecker et al 1990) and the import of fresh water and sea ice from the Arctic (Aagaard & Carmack 1989).

The salty Mediterranean outflow at middepth contributes to the high salinity of the near-surface layer of the Norwegian Sea (Reid 1979), preconditioning it for deep convection. The only marginal sea that could provide a similar mechanism in the Pacific is the Sea of Okhotsk on the western side of the basin. Although the outflow of Mediterranean water does not contribute directly to NADW (since entrainment during descent along the continental slope reduces its density through mixing with thermocline water), it can influence the density within the Labrador Sea and Norwegian Sea overflow regions (Warren 1981). Vertical mixing of the saline waters may therefore contribute to the high-latitude Atlantic salinity (Reid 1979) and precondition waters for convection in the Labrador and GIN Seas. A recent series of hydrographic measurements within the Sea of Okhotsk (H Freeland, personal communication) found that water properties exhibit a maximum density (owing to cold winter outbreaks) at a salinity of 32.94 to 33.08 psu (densities of 26.51 to 26.62 σ_θ) which is not

high enough to allow deep convection below the upper several hundred meters of the water column.

A number of climate modeling studies have been conducted to investigate the stability of the present North Atlantic thermohaline circulation with respect to freshwater export from the Atlantic. One of the first such studies (Manabe & Stouffer 1988) demonstrated multiple equilibria in a fully coupled ocean-atmosphere model. Their first state was similar to the present climate, with active NADW production, while their second state had upwelling in both the Atlantic and Pacific. The surface freshwater flux difference between the cases indicates a roughly 0.1 m/yr freshening of the entire North Atlantic. Stocker & Wright (1991) have also identified these states in a zonally averaged coupled ocean-atmosphere model. Through a sensitivity analysis of the Atlantic-to-Pacific atmospheric freshwater transport, they showed that a cessation of NADW production occurred in their coupled model when the net interbasin atmospheric freshwater transport dropped to about 0.03 Sv (from the Atlantic to the Pacific). Once stopped, it took an increase of interbasin freshwater transport to 0.36 Sv before NADW production once more resumed. A similar hysteresis behavior was found by Rahmstorf (1995) through his analysis of the effects of imposed surface freshening to the high-latitude North Atlantic Ocean. In particular, he found that the addition of a perpetual 0.06 Sv freshening (about a quarter of the discharge rate of the Amazon River) to the North Atlantic led to an irreversible shutdown of the conveyor. None of these studies, however, found the occurrence of NPDW, even upon the total shutdown of NADW.

Two notable modeling studies have been able to generate NPDW formation within their parameter sensitivity analyses. In the first of these, Stocker et al (1992), using a zonally averaged ocean model coupled to an energy balance model with a parameterization of the hydrological cycle, found the inverse conveyor belt (with NPDW formation and no NADW formation) as a possible equilibrium solution. Without the inclusion of parameterized wind forcing, this equilibrium tended to occur only under relatively large Atlantic-to-Pacific interbasin atmospheric freshwater transports and relatively large freshwater flux perturbations into the North Atlantic. When wind forcing was included, NPDW states were possible under a wider range of allowable interbasin freshwater transports, although similar large local freshening in the North Atlantic was also required. Hughes & Weaver (1994) also undertook a detailed sensitivity study using an ocean GCM to specifically address why the present-day Pacific Ocean did not form deep water. Under present-day geometry and forcing, there was a clear preference for their model to end up in a conveyor belt scenario (with NADW and AABW formation and no NPDW formation), starting from a variety of initial conditions. It was also possible to realize the second solution (with AABW formation and no NADW or NPDW formation) of Manabe &

Stouffer (1988). Studies of the sensitivity of model solutions to the width of the basin, the northern extent of the Atlantic, the length of southern tip of South America (relative to Africa), and a reduction in the Southern Hemisphere winds all allowed possible equilibria (under present-day boundary conditions) with NPDW formation. Although they were not able to point to a single factor in determining the cause of a lack of NPDW formation in the present climate, they were able to show quantitatively that in cases where NPDW did occur (under changed geometry or wind forcing), the meridional surface density and depth-integrated steric height gradients from the high-latitude North Pacific to the high-latitude South Pacific reversed.[2]

It is clear from this subsection that the question of why deep water forms in the Atlantic and not in the Pacific is far from being resolved. While it is apparent that in the present climate it is due to the fact that the North Pacific is much fresher than the North Atlantic, this in itself is not independent of the existing thermohaline circulation. Nevertheless, it is clear that NPDW can be initiated if processes occur that reverse the present-day basin-scale depth-integrated steric height gradient along the western boundary of the Pacific Ocean. That is, since the large-scale surface meridional flow in both the Pacific and Atlantic Oceans is down the basin-scale meridional depth-integrated steric height gradient (in a frictional western boundary layer) (Hughes & Weaver 1994), processes that can change this gradient control whether deep water formation occurs or does not occur in a particular basin. These processes could occur in either the Northern Hemisphere (e.g. changes in high northern latitude evaporation minus precipitation or Arctic freshwater discharge) or Southern Hemisphere (e.g. changes in the intensity of southern winds).

INTERACTION BETWEEN THE ARCTIC AND THE HIGH-LATITUDE OCEANS

In this section we review the interactions between the Arctic and the North Atlantic and Pacific. We begin by addressing oceanic interactions between the Arctic and the North Atlantic, through the exchange of waters through Fram Strait, Barents Sea, and the Canadian Archipelago and subsequently between the Arctic and the North Pacific via exchanges through the Bering Strait. We then discuss atmospheric interactions between the high-latitude oceans and the Arctic. Owing to the sensitivity of deep convection in the North Atlantic to changes in salinity, a whole subsection is devoted to the freshwater budget of the Arctic.

[2]Steric height gives a measure of the height difference between two isobaric surfaces in the ocean. Gradients in depth-integrated steric height (from an assumed level of no motion to the surface of the ocean) give a measure of upper-ocean mass transport.

Ocean Circulation

This section is partitioned into two parts specifically dealing with the interactions between the North Atlantic and the Arctic and the North Pacific and the Arctic. These interactions are summarized in Figure 2, which shows the oceanic exchanges between the Arctic and high-latitude oceans.

ARCTIC/NORTH ATLANTIC INTERACTIONS The deepwater formation regions of the northern North Atlantic are delicately poised in their ability to sustain convection (Aagaard & Carmack 1989). Because density is largely a function of salinity at low temperatures, a moderate freshening of the surface waters of the North Atlantic could impact deepwater formation and cause a freshwater capping of these regions, leading to a cessation or reduction of deep-water formation. This is one means by which the waters of the North Atlantic are modified through ocean interactions with the Arctic. Additionally, the North Atlantic has a large influence on the import of heat, mass, and salinity into the Arctic Ocean. This has consequences for the stability of the Arctic ice pack.

The Arctic and North Atlantic Oceans communicate directly through the relatively deep (approximately 2500 m deep) Fram Strait, which runs between northeast Greenland and Spitsbergen at approximately 80°N latitude. The West Spitsbergen Current (WSC) brings about 3 to 5 Sv of relatively warm, saline water, with a temperature of approximately 3°C and salinity of 35 psu, northward along the western side of Spitsbergen into the Arctic Ocean. Observations suggest that the maximum transport of the WSC occurs during winter (Morison 1991). As this warm water flows around the Greenland Sea, it is cooled dramatically. Approximately 350 W m^{-2} of heat is lost to the atmosphere, whereas another 200 W m^{-2} or so is lost in the process of melting sea ice which originated in the Barents Sea (Boyd & D'Asaro 1994). The relative strength of these processes influences the density of the water column, with atmospheric cooling resulting in cold and saline water that is capable of sinking to great depths and ice melt causing much fresher and hence stable surface waters.

The WSC appears to split into a number of different branches at the Yermak Plateau just northwest of Spitsbergen (e.g. Quadfasel et al 1987, Aagaard et al 1987). The western section of the current recirculates into the Fram Strait, whereas the remainder of the water moves northward along the shelf break into the Arctic Ocean. It is estimated that only 20 to 30 percent of the WSC continues to the Arctic Ocean, with the remaining 70 to 80 percent recirculating into the Greenland Sea (e.g. Buorke et al 1988, Manley 1995). This recirculated water is relatively dense and is likely an important contributor to the formation of deep water. The northward flowing branch sinks below the relatively fresh polar surface water and makes up a portion of the Atlantic layer, which is observed in the Arctic basin between 200 and 800 m. This layer represents a

large reservoir of heat and is identified by a subsurface potential temperature maximum with relatively high salinity. The impact of this water on Arctic sea ice is mitigated by a layer of fresh surface water that stabilizes the water column and reduces the upward heat flux. As discussed below, this surface water is largely maintained by river runoff and the inflow of fresh water from the Pacific Ocean through the Bering Strait.

In addition to the WSC the Atlantic layer in the Arctic is fed by waters that flow into the Arctic through the Barents and Kara Seas (e.g. Rudels et al 1994). This water flows northward to the east of Spitsbergen over the relatively shallow (400 to 500 m) Bear Island Trough. It is modified on the shelves of the Barents Sea through the mixing of river runoff with shelf waters, heat loss to the atmosphere, and sea ice processes. As a result, the Atlantic layer is colder and fresher than the modified Atlantic water that flows through the Fram Strait. The two branches of Atlantic water meet at the shelf break of the Kara Sea. Recent modeling studies (Gerdes & Schauer 1997) suggest that the Barents Sea branch is the most important in terms of the inflow of heat, mass, and salinity into the Arctic Ocean. The strength and variability of this inflow have consequences for ice formation on the shelf regions and the water mass structure within the Arctic. Recent observations (e.g. Carmack et al 1995, McLaughlin et al 1996) indicate that the Atlantic layer within the Arctic Ocean has undergone large changes since 1990. These include a shift in the frontal structure, which separates different Atlantic layer water masses (from the Lomonosov ridge to the Mendeleyev ridge (Figure 2)), and a significant warming of the Atlantic layer. By 1994, this warming extended across the Nansen, Amundsen, and Makarov Basins. Swift et al (1998) show that these changes are likely caused by an increase in the temperature of the Atlantic waters that enter the Arctic Basin through Fram Strait. The anomalous warmth of these waters appears to be correlated with the North Atlantic Oscillation (NAO), which corresponds to relatively warm air temperatures in the Greenland Sea region and thus a reduction in oceanic heat loss. The temperature signal of these waters is transported into the Arctic Ocean by topographically steered boundary currents. It then enters the interior ocean through intrusive layers that extend laterally into the ocean basins (Carmack et al 1998). The question remains open as to where the Arctic waters displaced through the intrusion of the Atlantic layer went, although enhanced transport through the Canadian Archipelago is plausible. This would be consistent with recent observations of anomalous cold and fresh waters in the Labrador Sea since the late 1980s (Dickson et al 1996).

The East Greenland Current (EGC) represents the primary outflow of water from the Arctic Ocean. It transports sea ice as well as surface, intermediate, and deep water southward through Fram Strait along the eastern coast of Greenland. The surface waters of this current are made up of relatively cold ($<0^{\circ}$C) and

fresh (salinity below 34.4 psu) polar water. The recirculated water from the WSC sinks below the surface water and moves southward with the EGC (e.g. Swift & Aagaard 1981). A wide range of transport estimates exists for the EGC (see Carmack 1990). At approximately 72°N a portion of the current branches eastward, resulting in a net cyclonic circulation within the Greenland Sea. The remainder of the EGC continues southward along the Greenland coast.

A complicated series of relatively shallow (less than 400 m) channels make up the Canadian archipelago. Fissel et al (1988) estimate that 1.7 Sv of Arctic surface water is transported through this region into Baffin Bay (see also Aagaard & Carmack 1989). This water is relatively fresh, and variability in its outflow may impact the deep-water formation that occurs in the Labrador Sea region, as discussed earlier.

ARCTIC/NORTH PACIFIC INTERACTIONS The high-latitude North Pacific exchanges surface waters with the Arctic Ocean through the shallow (50 m deep) Bering Strait. This strait (by way of the Arctic Ocean) is one of only two ways in which the Pacific and Atlantic Oceans are connected (the other being via the ACC), suggesting that changes in the relatively fresh Bering Strait inflow may influence NADW formation (e.g. Wijffels et al 1992). Box model studies (Shaffer & Bendtsen 1994) have suggested that the stability of the thermohaline circulation in past climates may have been influenced by the mean transport (or lack thereof) of Pacific waters through the Bering Strait.

In the present climate, approximately 0.8 Sv is transported northward through Bering Strait. This inflow is driven by an approximately 0.5 m decrease in sea level between the Pacific and North Atlantic (e.g. Stigebrandt 1984, Overland & Roach 1987). Its variability is largely tied to the meridional wind field in the region (Aagaard et al 1985a, Coachman & Aagaard 1988). For example, Roach et al (1995) show that under strong (10 to 12 m s^{-1}) sustained northerly winds the Bering Strait flow can temporarily reverse, bringing Chukchi Sea water southward. The Pacific water that is transported into the Arctic Ocean is relatively fresh, with a salinity of approximately 32.5 psu. Seasonal and interannual variability in the transport and salinity of this inflow is high (e.g. Roach et al 1995).

Atmospheric Circulation

The Arctic atmosphere acts as heat sink for the Northern Hemisphere through radiative cooling to space. According to Nakamura & Oort (1988), when averaged annually, 98 percent of the energy needed to balance radiative cooling at the top of the atmosphere from 70° to 90°N enters the Arctic through the poleward convergence of atmospheric heat transport. The remaining two percent is supplied by the underlying surface, suggesting that the poleward oceanic transport of heat and export of ice contribute little to the Arctic atmosphere's

energy budget. Nakamura & Oort (1988) showed that the largest contribution to the atmospheric energy transport is from transient eddies, with stationary eddies also making a significant contribution during the winter. Their analysis was later extended by Overland & Turet (1994) and Overland et al (1996), who found the major pathways of heat transport are over the Greenland, Barents, and East Siberian Seas.

Although the annually averaged net flux of heat from the atmosphere to Earth's surface is small, the annual variations are at times comparable to the atmospheric energy transport into the Arctic region (Oort 1974, Nakamura & Oort 1988, Overland & Turet 1994). Based on calculations by Maykut (1982), the net flux from the atmosphere to the underlying surface (averaged over sea ice and open water) in the central Arctic ranges from 75 W m^{-2} in July to -25 W m^{-2} in November–December. Analysis of observations by Vowinckel & Orvig (1971) indicates that the surface energy budget is controlled by advection in the winter and by solar radiation in the spring and summer. Ultimately, the energy exchanged with the atmosphere at the surface influences the mass of sea ice, resulting in approximately a 1 m annual range of the area-averaged thickness in the Arctic Basin.

Recent interest has focused on how the high-latitude atmospheric circulation influences sea ice motion (e.g. Walsh & Johnson 1979, Overland & Pease 1982, Serreze et al 1989, Fang & Wallace 1994), including the export of ice from the central Arctic to the Greenland Sea (Mysak et al 1990, Walsh & Chapman 1990) and the distribution of heat and moisture at high latitudes (Serreze et al 1995, Overland et al 1996). The mean Arctic winter sea-level pressure (SLP) is characterized by high-pressure centers over the Beaufort Sea and Greenland and a ridge over Siberia (Figure 9*a*) associated with the extremely low temperatures in these regions (Figure 10). The mean summer SLP distribution is quite flat, with a weakened Beaufort high shifted toward Canada from its wintertime position. Ice motion, shown with SLP in Figure 9 follows the anticyclonic wind stress along the Beaufort gyre and transpolar drift from Siberia through Fram Strait and into the Greenland Sea. The interaction of the jet stream with the northern Rocky Mountains creates a stationary wave structure, resulting in the polar stratospheric vortex, which is seen extending into the troposphere at the 500-mbar level in Figures 9*b* and 9*d*.

Winter cyclonic activity is most common south of Iceland and often moves along the ice edge into the Norwegian, Barents, and Kara Seas (Whittaker & Horn 1984, Serreze et al 1993). Summer cyclones are generally weaker, less frequent, and more broadly distributed.

NORTH ATLANTIC Observations of strong decadal variability in the North Atlantic SST and atmospheric circulation have prompted many studies to seek

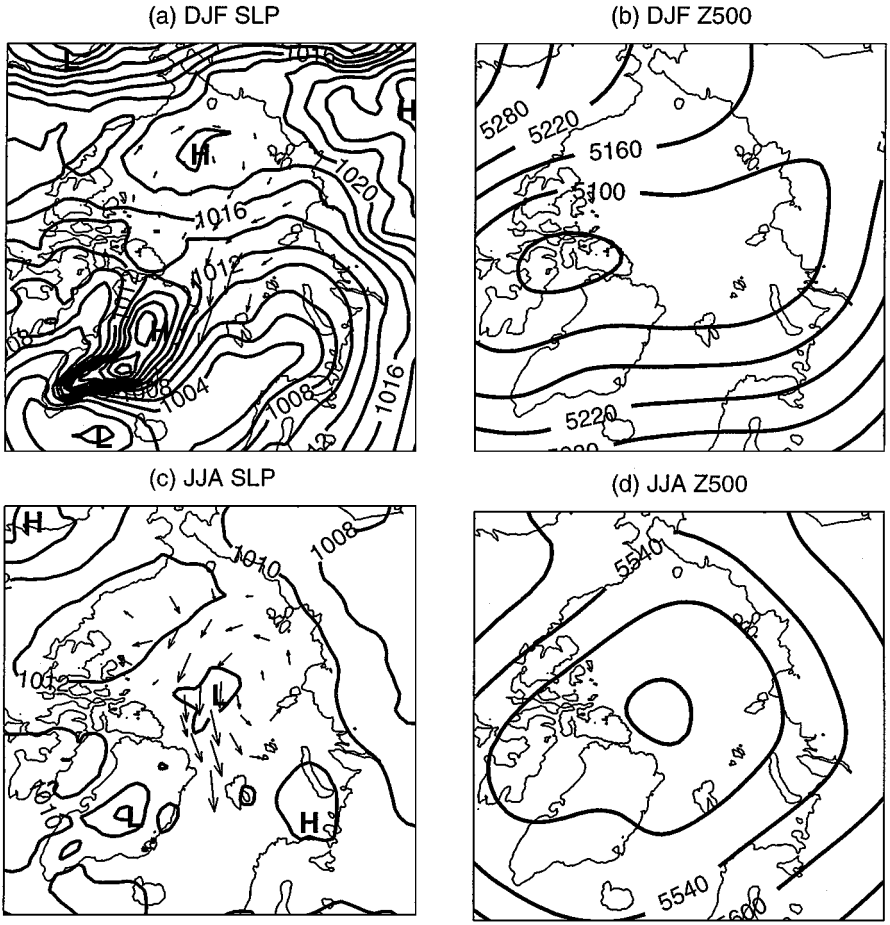

Figure 9 Mean sea level pressure (SLP) and 500 mbar height (Z500) for winter (December-January-February—DJF) and summer (June-July-August—JJA) from National Center for Atmospheric Research/National Center for Environmental Prediction (NCAR/NCEP) reanalysis data 1958–1997 provided through the NOAA Climate Diagnostics Center. Mean sea ice drift vectors for winter and summer 1979–1996 are shown with SLP. The drift speed in Fram Strait is 6.8 (3.0) cm/s in winter (summer). Ice drift data are provided by the International Arctic Buoy Programme.

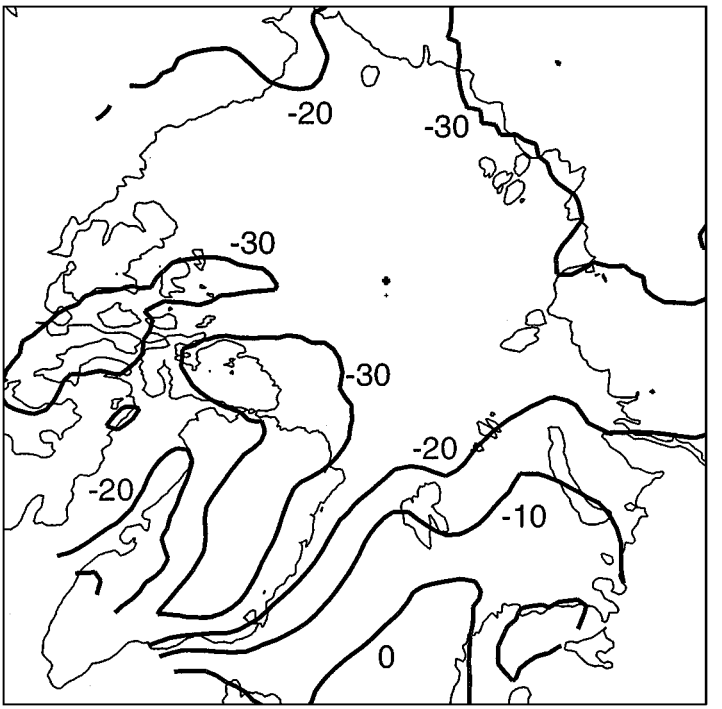

Figure 10 Winter (December-February) mean 2 m air temperature from the International Arctic Buoy Programme and the Polar Exchange at the Sea Surface Project (Martin & Munoz 1997).

linkages between the North Atlantic and Arctic climate systems. Here we focus on relationships established through the atmosphere. Investigations by Wallace & Gutzler (1981) and Barnston & Livezey (1987) showed that the dominant atmospheric circulation pattern in the North Atlantic is the North Atlantic Oscillation (NAO), a north-south oscillation in atmospheric mass with centers of action near Iceland and the Azores as defined by Walker & Bliss (1932). Fluctuations of the NAO have been linked to surface air temperature (SAT) anomalies in northern Europe and the northwestern Atlantic (van Loon & Rogers 1978), precipitation anomalies in Europe and over the Labrador Sea (Hurrell 1995), sea ice conditions in the Atlantic sector (Rogers & van Loon 1979, Walsh & Johnson 1979, Fang & Wallace 1994), sea ice export through Fram Strait (R. Dickson and D. Rothrock, personal communication), and the distribution of cyclones (Rogers 1990, Hurrell 1996, Serreze et al 1997). Figure 11 shows the NAO index and the signature of the NAO on SLP based on compositing years with strongly positive and negative NAO indices. The positive polarity of the NAO

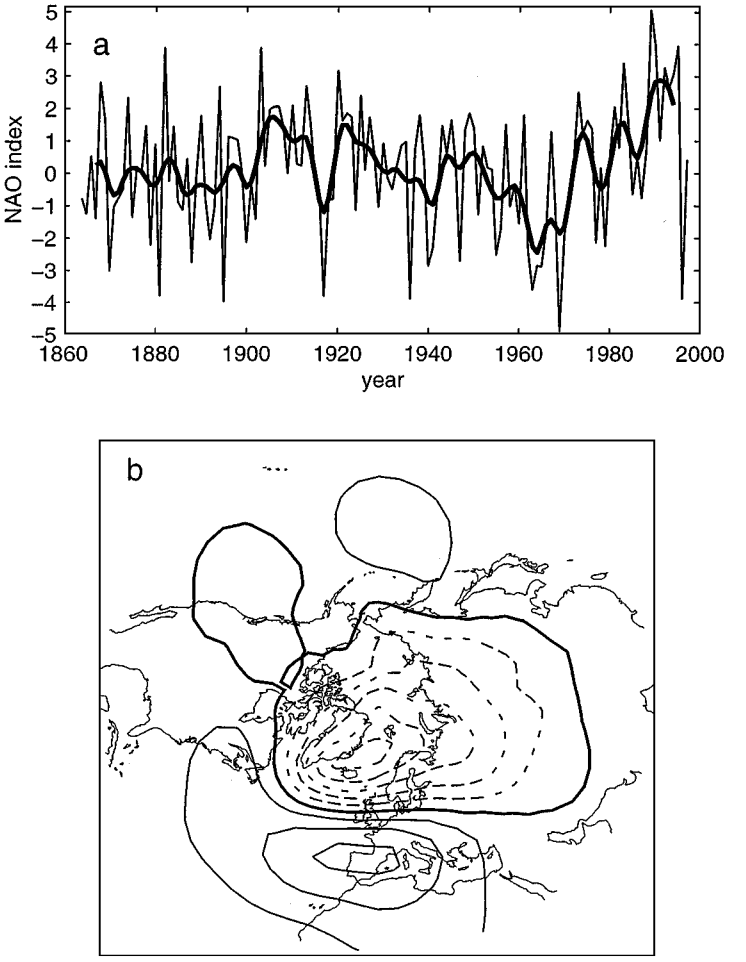

Figure 11 (*a*) Winter (December-March) index of the NAO based on the pressure difference between Lisbon, Portugal, and Stykkisholmur, Iceland, normalized by division of each seasonal pressure by the long-term (1864–1983) standard deviation. The heavy solid line shows the index filtered to remove variability with periods less than 4 years. (*b*) The SLP composite difference (high minus low) since 1899 for years with NAO index exceeding ± 1. Contours are drawn at 2 mbar intervals, negative contours are dashed, and the zero contour is a heavy solid line. (Figure 11*b* is modeled after Figure 1 in Hurrel 1995, with the addition of data through 1997.) The index is provided by the NCAR climate analysis section and differs from that of Hurrel (1995) only in the base period used for normalization (Hurrel used 1964–1994).

is characterized by a broad high-pressure center in the North Atlantic near 40°N and 30°W and a more spatially confined low centered over Greenland.

One of the primary ways in which the atmospheric circulation affects Arctic-North Atlantic interactions is via its direct and indirect forcing on sea ice in these regions. The links between atmospheric circulation and sea ice conditions in the Davis Straits and Labrador Sea regions are well known. Rogers & van Loon (1979) found that below normal temperatures in Greenland (or positive polarity of the NAO) are associated with heavy ice conditions in the Davis Strait and near Newfoundland, and light ice conditions in the Baltic Sea in winter and the following spring. Using an empirical orthogonal function (EOF) analysis of sea ice extent in the North Atlantic for all seasons from 1953 through 1977, Walsh & Johnson (1979) found the leading EOF corresponds to heavy ice in the Davis Straits/Labrador Sea and light ice in the Barents Sea. The pattern of sea ice extent is correlated with the leading EOFs of atmospheric variability from monthly anomalies of SLP, surface temperature, and 700 mbar heights and temperature. Lagged cross correlations suggest that during autumn the strength of forcing between sea ice and atmosphere is comparable. However, during summer, ice conditions are influenced by atmospheric forcing for a longer lead time.

Much has been written recently about a pattern of variability consisting of a dipole in the wintertime sea ice concentration between the Davis Straits/Labrador Sea region and the Greenland/Barents Sea (Mysak et al 1990, Fang & Wallace 1994, Slonosky et al 1997). For the winters of 1972 through1989, Fang & Wallace (1994) found that the sea ice dipole pattern is strongly coupled to the NAO such that the positive polarity of the NAO is observed with positive sea ice anomalies in the Davis Straits/Labrador Sea. They examined the data at seven-day intervals and determined that the relationship is strongest when the atmosphere leads the ice by two weeks. The negative polarity of the NAO is associated with blocking (diminished westerly flow) in the Greenland region, which Fang & Wallace (1994) link with a retreating (advancing) ice edge in the Davis Straits/Labrador (Greenland/Barents) Sea. Focusing on interannual variability, Slonosky et al (1997) show that a similar dipole pattern of wintertime sea ice anomalies for 1954–1990 is strongly correlated with atmospheric anomaly fields for simultaneous periods and for sea ice leading the atmosphere by one year. Positive sea ice anomalies are seen with high pressure over Greenland, Iceland, and the Canadian Archipelago.

Sea ice concentration anomalies in the Davis Straits/Labrador Sea region and Greenland/Barents Sea region are plotted in Figure 12*a*. Strong decadal features are present in the Labrador Sea as discussed by Mysak & Manak (1989) and Deser & Blackmon (1993). The tendency for area anomalies in the two regions to be out of phase is evident, particularly in the last half of the record. The cross correlation in Figure 12*b* reveals a significant negative correlation at zero

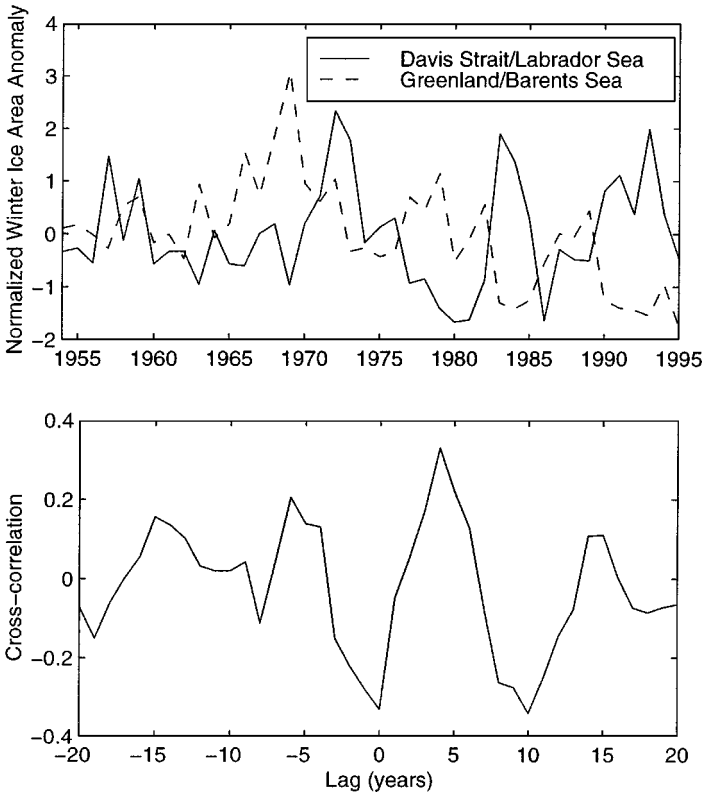

Figure 12 (*a*) Normalized wintertime (November to March) sea ice area anomalies in the Davis Straits/Labrador Sea region and Greenland/Barents Sea region and (*b*) cross correlation of the time series. The data are normalized by the standard deviation and are plotted in the year in which January occurs. Positive lag refers to anomalies in the Davis Straits/Labrador Sea lagging those in the Greenland/Barents Sea. The Davis Straits/Labrador Sea (Greenland/Barents Sea) region is defined as the area from 45°–65°N and 45°–70°W (65°–78°N and 25°W–60°E). Data were kindly provided by National Snow and Ice Data Center User Services and compiled by Walsh & Chapman.

lag. As noted by Mysak et al (1990), the strongest correlation occurs when area anomalies in the Davis Straits/Labrador Sea lag those in the Greenland/Barents Sea region by four years. The recurrence of a significant negative correlation at 10-year lag is evidence of the strong decadal variability relating ice anomalies in these regions.

Mysak & Manak (1989) discussed the propagation of sea ice anomalies from the Greenland Sea to the Labrador Sea over a period of approximately four years. In particular, they highlight the movement of the 1968 Greenland Sea

anomaly associated with the Great Salinity Anomaly (GSA). Inspired by the strong decadal signal, Mysak et al (1990) gathered evidence in support of an interdecadal self-sustained climate cycle in the Arctic. The proposed negative feedback connects decreased cyclogenesis in the high-latitude atmosphere to positive sea ice anomalies in the Greenland Sea. Decreased storminess ultimately leads to higher salinity in the Arctic Ocean owing to a lack of precipitation and runoff. Finally, high-salinity water decreases the sea ice extent in the Arctic and Greenland Sea leading to the inverse process.

Wohlleben & Weaver (1995) proposed a modified version of the Mysak et al (1990) climate cycle that eliminates the connection between anomalous river runoff and sea ice extent in the central Arctic. Instead, they argued that deep convection in the Labrador Sea creates positive SST in the subpolar gyre, which enhances sea-level pressure over Greenland and weakens the Icelandic low (i.e. negative polarity of NAO) through the modification of storm tracks. Anomalous northerly winds enhance the transport of ice and fresh water as a result of the reduced east-west pressure gradient at high latitudes. Finally, these ice and freshwater anomalies are swept into the subpolar gyre and eventually reach the Labrador Sea, where they weaken convection and begin the inverse process.

It is possible that these feedback cycles may help explain why observations show that strong decadal variability in the sea ice extent in the Labrador Sea leads SST anomalies east of Newfoundland by two years (Deser & Blackmon 1993). Furthermore, these feedback cycles suggest that such diverse interactions as the GSA and the large-scale changes that have been seen in the northern North Atlantic are not simply explained. For example, there is observational (Walsh & Chapman 1990) and modeling (Häkkinen 1993) evidence to support the idea that ice and freshwater export were anomalously strong prior to the GSA of the late 1960s when the Icelandic Low was anomalously weak (negative polarity of the NAO, see Figure 11*a*). However, recent studies show that the relationship between NAO and ice export appears to have changed sign in the last two decades, such that export is positively correlated with the NAO (R. Dickson and D. Rothrock, personal communication). In the past two decades we have seen a strong positive NAO pattern leading to enhanced export and decreased ice concentration in the Greenland Sea. Hence the sea ice must have melted at an extraordinary rate in the Greenland Sea for the past 20 years. It is thought that this might contribute to the sustained weak convection seen in the Greenland Sea since the mid-1970s.

NORTH PACIFIC Interaction between the northern North Atlantic and the Arctic appears to be a two-way process, including the transport of heat and moisture to high latitudes by the atmosphere, the exchange of fresh water between the

Arctic and the North Atlantic, and the modulation of air-sea exchange by sea ice anomalies. However, studies of interactions in the northern North Pacific sector suggest primarily that large-scale atmospheric circulation forces a local response in sea ice anomalies.

Overland & Pease (1982) determined that the maximum wintertime sea ice extent in the Bering Sea is strongly correlated with the difference in the number of cyclone centers in the eastern and western parts of the northern Pacific Basin. Sea ice advance is inhibited by southerly winds associated with storms traveling along the western side of the Bering Sea. Rogers (1981) showed that the position of the ice edge in the Bering is linked to the strength of the north-south temperature gradient, which he associated with an atmospheric teleconnection pattern he called the North Pacific Oscillation after Walker & Bliss (1932). Analogous to their results in the North Atlantic, Fang & Wallace (1994) found a dipole pattern in the Pacific sector with opposing centers of action in the Bering Sea and the Sea of Okhotsk. They associated the advance (retreat) of ice in the Sea of Okhotsk (Bering Sea) with a blocking ridge in the Gulf of Alaska.

Freshwater Budget

Because water density is largely controlled by salinity at low temperatures, the freshwater exchange between the Arctic and high-latitude oceans is very important in determining the strength of the thermohaline circulation. Relatively small changes in the flux of freshwater to the convective regions are likely to significantly affect NADW formation (e.g. Aagaard & Carmack 1989). The freshwater flux between the Arctic and North Atlantic is made up of both ocean and sea ice transports. The Arctic freshwater budget is also important for the stability of the water column in the Arctic and the insulation of sea ice from the relatively warm subsurface Atlantic water.

The freshwater budget of the Arctic Ocean has been discussed by Aagaard & Carmack (1989). The primary freshwater input to the Arctic Ocean is river runoff. Approximately 10 percent of the world's river runoff, accounting for approximately 3300 $km^3\ yr^{-1}$, enters the Arctic Ocean, which occupies only 5 percent of the total ocean surface area and 1.5 percent of its volume.

Large seasonal and interannual variability exists in the river runoff (Cattle 1985). Bering Strait inflow represents the second largest freshwater source for the Arctic Ocean ($\sim$1670 $km^3\ yr^{-1}$), with precipitation minus evaporation ($\sim$900 $km^3\ yr^{-1}$) and the import of fresh water in the Norwegian coastal current ($\sim$330 $km^3\ yr^{-1}$) accounting for the remainder of the freshwater sources. These large inputs of fresh water allow the Arctic surface waters to remain relatively fresh ($<$34.4 psu), which results in a stable water column and the isolation of sea ice from the heat associated with the Atlantic layer of the Arctic.

The sources of fresh water for the Arctic are balanced primarily by the export of sea ice (which has a salinity of approximately 3 psu) in the East Greenland Current (EGC), which accounts for a freshwater loss to the Arctic and a gain by the Greenland Sea of approximately 2800 km^3 yr^{-1} (Aagaard & Carmack 1989). The exchange of water through the Canadian Archipelago and Fram Strait results in a loss of approximately 900 km^3 yr^{-1} and 820 km^3 yr^{-1} of fresh water, respectively. The variability in these outflows has important consequences for the deep-water formation that occurs in the GIN and Labrador Seas. For example, modeling results from Mauritzen & Häkkinen (1997) show that the thermohaline circulation increased by 10 to 20 percent in response to a decrease in sea ice export of 800 km^3. The relative strength of the freshwater sources to the GIN and Labrador Seas from the Arctic will also likely influence the preferred location and relative strengths of deep-water formation. From a relatively short time series (1979 to 1985), Steele et al (1996) show that simulated interannual variability in the outflow through the Canadian Archipelago is anticorrelated to the outflow through Fram Strait, with the Fram Strait anomalies leading the Canadian Archipelago anomalies by one year. This may explain why deep-water formation in the GIN and Labrador Seas has been observed to be out of phase in the past few decades.

The large changes that occur in Arctic/North Atlantic freshwater exchange are epitomized by the GSA of the late 1960s. This event freshened the upper 500 m of the northern North Atlantic with a freshwater excess of approximately 2000 km^3 (or 0.032 Sv over a two-year period). Dickson et al (1988) trace this freshwater anomaly as it was advected around the subpolar gyre for more than 14 years. It originated north of Iceland in the late 1960s, moving southwestward into the Labrador Sea (1971 to 1973) and then proceeding across the North Atlantic, returning to the Greenland Sea in 1981 to 1982.

Several studies have examined the cause of the GSA and have generally determined that it was a result of Arctic/North Atlantic interactions. Both modeling (Häkkinen 1993) and observational (Walsh & Chapman 1990, Wohlleben & Weaver 1995) studies concluded that strong northerly winds caused an increased sea ice export into the Greenland Sea. The large freshwater flux anomaly that was associated with this transport was likely enhanced by the relatively large advection of thick ice from north of Greenland. Additionally, as simulated by Häkkinen (1993), increased oceanic transport of fresh water from the Arctic occurred. This was caused by fresh anomalies within the Siberian Sea that were advected across the Arctic, entering the Greenland Sea approximately 4 years later. During the GSA the anomalous sea ice and oceanic freshwater transports were coincident, resulting in a significant and persistent freshening of the North Atlantic. This freshening appears to have resulted in a reduction of deepwater formation with winter convection in the Labrador sea limited to

the upper 200 m (compared with 1000 to 1500 m for 1971 to 1973) (Lazier 1980).

DECADAL-INTERDECADAL VARIABILITY

In this section we discuss observational evidence concerning the existence of decadal-interdecadal variability in the North Atlantic and Pacific Oceans. An attempt is made to link analytical and numerical studies with observational data. More comprehensive reviews of this topic are given by Anderson & Willebrand (1996) and Latif (1998).

The Atlantic

North Atlantic SST records for the past century reveal slowly varying basin-scale changes including cold anomalies prior to 1920, warming from 1930 to 1940 and cooling again in the 1960s. Kushnir (1994) described the SST pattern associated with these long-term changes as unipolar (see Figure 13) with a strong maximum around Iceland and in the Labrador Sea and a weaker maximum in a band near 35°N across the central Atlantic. The atmospheric pattern associated with the cooling in the 1960s has a negative pressure anomaly to the east of positive SST anomalies (also see Deser & Blackmon 1993, who suggest that the pattern resembles the NAO). Because the SLP anomalies appear downstream of the SST anomalies, Deser & Blackmon suggest that the atmosphere is responding to the ocean on these timescales.

Evidence for changes in the subpolar North Atlantic Ocean over similar timescales, compiled by Dickson et al (1996), indicates that synchronous with the cooling in the late 1960s, convective activity reached a maximum in the Greenland Sea and a minimum in the Labrador Sea. These convective extremes occurred at the approximate time of the GSA. Since the early 1970s, the Greenland Sea has become progressively more saline and warmer through horizontal exchange with the deep waters of the Arctic Ocean. At the same time, the Labrador Sea has become colder and fresher as a result of local deep convection. Further signs of internal ocean dynamics can be seen in propagating signals of temperature and salinity. Hansen & Bezdek (1996) found temperature anomalies that remain coherent for 3 to 10 years circulating along the subpolar and subtropical gyres. Because the anomalies move slower than the near-surface ocean circulation, they speculated that the motion could be influenced by ocean wave activity. Reverdin et al (1997) explored patterns associated with salinity anomalies and found that a single pattern explains 70 percent of the variance of lagged salinity anomalies. The pattern represents a signal originating in the Labrador Sea that propagates from the west to the northeast in the subpolar gyre. The strong correlation between salinity and sea ice in the Labrador Sea

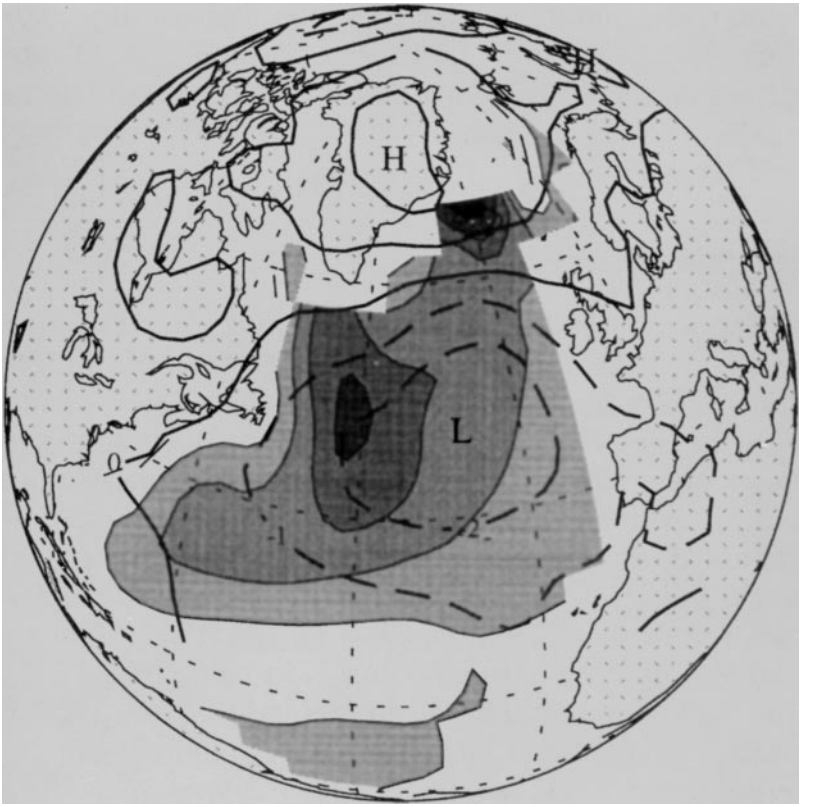

Figure 13 Composite differences of winters (December-April) 1950–1964 and 1970–1984. SLP is contoured with *heavy lines* at 1 mbar intervals, and SST is contoured with shaded regions separated by light lines at 0.2°C intervals. *Dashed lines* indicate negative values (from Kushnir & Held 1996).

led Reverdin et al (1997) to link the salinity anomalies to the export of Arctic fresh water.

The short and sparse record of oceanographic measurements, and the complicated nature of the interactions involved, motivate the use of models to clarify the processes associated with decadal variability. It is possible for ocean-only models (e.g. Weaver & Sarachik 1991) to exhibit internal variability on decadal timescales in their thermohaline structure when forced with mixed boundary conditions (i.e. SST is restored to a specified value and freshwater flux is prescribed). Low-frequency variability develops in these models when fluctuations in the thermohaline circulation are reinforced by salinity advection (a positive

feedback) and defeated by heat transport (a negative feedback that is somewhat confounded by using a restoring condition on SST). Because salinity variations control the stability of the water column in the northern North Atlantic, instabilities arise when a sufficiently strong local minimum in the freshwater forcing is prescribed near the sinking region (Weaver et al 1991, 1993). In addition, models with weak SST restoring exhibit more stable thermohaline circulations (Zhang et al 1993). With a zonally averaged ice-ocean model, Yang & Neelin (1993) identified another feedback mechanism for long-term thermohaline variability. They showed that ice melt decreases the near-surface salinity, thereby weakening the thermohaline circulation. In turn, the poleward heat transport is reduced, which causes sea ice growth and so leads to the inverse process.

Delworth et al (1993) described the first coupled ocean-atmosphere GCM study of long-term thermohaline variability. They associate the variability primarily with oceanic processes. Later, Delworth et al (1997) found that salinity anomalies in the surface layer of the Arctic Ocean precede anomalies of the thermohaline intensity by 10 to 15 years. In agreement with the proposed climate cycle of Wohlleben & Weaver (1995), these Arctic freshwater anomalies are connected to the North Atlantic through sea-level pressure anomalies in the Greenland Sea resembling the pattern that Walsh & Chapman (1990) report preceded the GSA. Weaver & Valcke (1998) give further evidence that the Geophysical Fluid Dynamics Laboratory model thermohaline variability is a mode of the fully coupled atmosphere-ocean-ice system.

If decadal variability in the North Atlantic is truly a coupled phenomenon, then it is essential to our understanding to determine how the atmosphere responds to midlatitude SST anomalies. Palmer & Sun (1985) examined this problem by using an atmospheric GCM with anomalous SST specified in the region 40° to 50°N and 40° to 60°W. Although weaker than the response to SST anomalies of similar magnitude in the tropics, Palmer & Sun (1985) found a wave train emanating from this SST anomaly region such that positive height anomalies were found downstream of positive SST anomalies in the model. Palmer & Sun (1985) and Wallace & Jiang (1987) showed that observations of atmospheric circulations based on SST anomalies in the same region verify the structure simulated in the model, although the amplitude of the response is about half as great. Similar modeling studies that explore the atmospheric response to midlatitude SST anomalies by Pitcher et al (1988), Ting (1991), Kushnir & Lau (1992), Lau & Nath (1994), and Kushnir & Held (1996) yield results somewhat contradictory to those of Palmer & Sun (1985). Recent studies by Peng et al (1995, 1997) attribute some of the discrepancies between these studies to differences in the basic state of the atmosphere upon initialization. Model resolution is another factor that seems to influence the atmospheric response to SST anomalies. Latif & Barnett (1994) found that the atmospheric response to Pacific midlatitude

SST anomalies is much stronger than the response reported by those mentioned above. They attribute the response to an unstable air-sea interaction.

Bjerknes (1964) described how air-sea interactions differ on interannual and interdecadal timescales. Based on evidence that annual mean SST and wind speed anomalies are negatively correlated, Bjerknes argued that interannual SST variability is mainly a response to fluctuations of atmosphere-ocean latent and sensible heat transfer. He suggested that the longer timescale variability was ocean based by linking the SST anomalies to changes in the ocean currents.

Recent analysis of more than a century of data by Deser & Blackmon (1993) and Kushnir (1994) lends support to many of the ideas of Bjerknes (1964). Deser & Blackmon (1993) identified two prominent modes of SST variability in the North Atlantic (see Figure 14). The leading EOF represents the long-term changes that were described in the first paragraph of this section (Figure 14*a*) and resembles the pattern Kushnir (1994) obtained by compositing different time periods (Figure 13). Higher frequency variability is evident in the second EOF (Figure 14*b*) with strong roughly two- and 10-year timescales for SST anomalies with opposing centers of action east of Newfoundland and southeast of the United States. Kushnir (1994) obtained a similar SST pattern by compositing anomalies based on interannual fluctuations.

The atmospheric pattern associated with the higher frequency SST mode (see Figure 15) is very different from that of the lower-frequency mode shown in Figure 13. Like SST, the SLP has a dipole structure that is somewhat displaced to the northeast of the SST pattern. The atmospheric circulation has anomalous westerly winds over negative SST anomalies and anomalous southerly winds over positive SST anomalies. As noted by Deser & Blackmon (1993) and Hurrell (1995), the local nature of this relationship is governed by changes in the oceanic mixed layer that result from wind-induced heat flux anomalies, in agreement with Bjerknes (1964).

The Pacific

Interannual variability in the Pacific Ocean is well known to be dominated by El Niño/Southern Oscillation (ENSO) variability and its associated teleconnection through the atmosphere to the North Pacific (Bjerknes 1969, Weare et al 1976, Horel & Wallace 1981, Wallace & Gutzler 1981, Deser & Blackmon 1995, Zhang et al 1997). Recently, however, it has become apparent that the North Pacific possesses its own rich modes of decadal-interdecadal variability (see reviews of Trenberth 1990 and Nakamura et al 1997). One of the most notable events in the North Pacific was the apparent climate regime change that occurred from late 1976 through 1988. During this period the SSTs in the central and western North Pacific Ocean were cooler than normal, whereas SSTs along the western coast of North America were warmer than normal and the Aleutian low

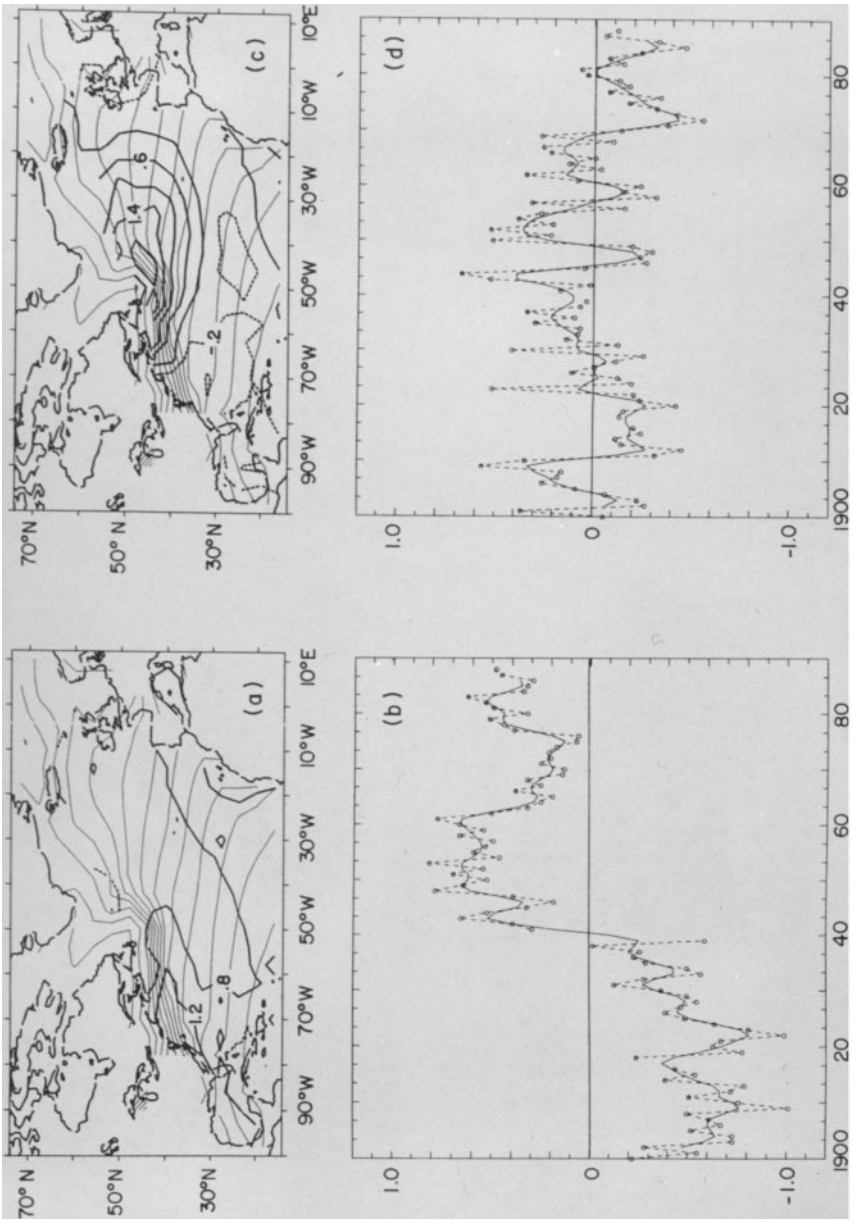

Figure 14 (*a*) Leading empirical orthogonal function (EOF) of winter mean (November–March) SST anomalies (*heavy lines*) and climatological winter mean (*light lines*) for the North Atlantic. (*b*) Expansion coefficient of EOF 1 (*dashed line*) and smoothed with a five-point binomial filter (*solid line*). (*c*) and (*d*) The same as Figures 14*a* and 14*b*, respectively, but for EOF 2. EOFs 1 and 2 account for 45 and 12 percent of the variance, respectively. (From Deser & Blackmon 1993.)

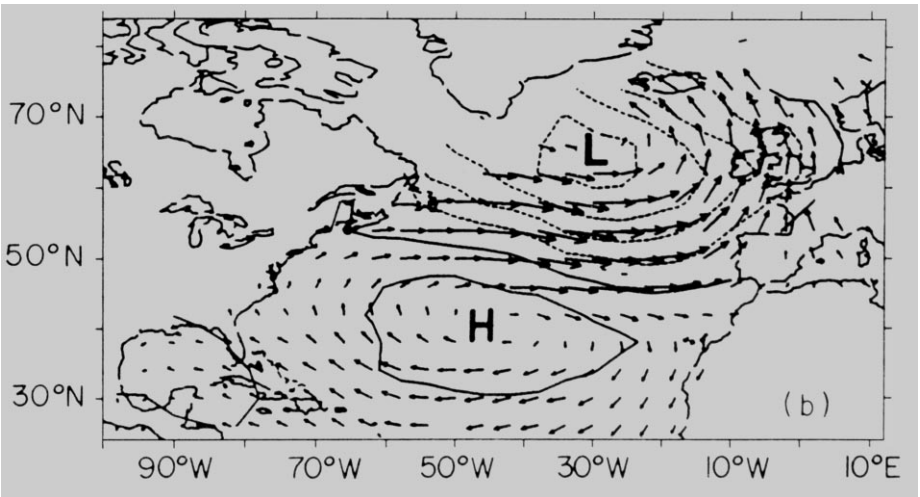

Figure 15 SLP and wind anomalies regressed on SST EOF 2, with opposite sign to the pattern shown in Figure 14*c* (from Deser & Blackmon 1993).

(see Figure 16) was deeper than normal (see Nitta & Yamada 1989, Trenberth 1990, Trenberth & Hurrell 1994). In attempting to explain this departure from normality, Trenberth (1990) pointed out that during this period there were three warm ENSO events with no intervening cold events (see Figure 17). Thus tropical temperatures were warmer than average, and so, through teleconnections to higher latitudes (Figure 16), the Aleutian low was deeper than normal on average. The end of this apparent regime change was marked by the strong cold event in 1989 (Figure 17). Subsequently, Trenberth & Hoar (1996) suggested that the 1990–1995 period was also anomalous in that tropical indices (see Figure 17) appeared to be locked into the warm phase. They described this "1990–1995 ENSO event" as the longest on record with a probability of occurrence about once every 2000 years. They further suggested the possibility that the ENSO changes may be partly caused by observed increases in greenhouse gases. Zhang et al (1997), on the other hand, provide compelling evidence to suggest that the 1976 "regime change" is by no means anomalous. They suggested that equally dramatic (but less studied) changes occurred around 1957 to 1958 (Figure 17). They further argued that the conditions during the 1977–1993 period were reminiscent of those that occurred from 1925 to 1942. Dettinger & Cayan (1995) and Zhang et al argued that regime changes are probably not the most informative way of characterizing decadal-interdecadal climate variability in the North Pacific.

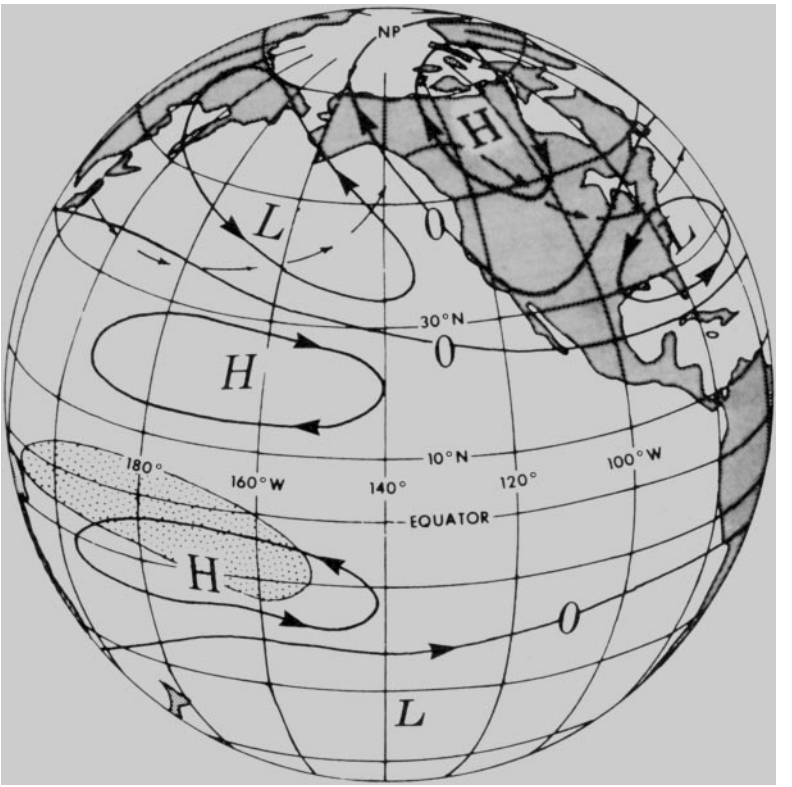

Figure 16 Diagram showing the Northern Hemisphere winter Pacific-North American (PNA) teleconnection pattern for warm SST anomalies in the equatorial Pacific Ocean (after Horel & Wallace 1981). The *wavy dashed line* with *arrows* lying between 30°N and 60°N shows a typical midtropospheric streamline that has been distorted by the anomaly pattern. The *shaded region* corresponds to where enhanced rainfall occurs in the equatorial band (redrawn from Mysak 1986).

Unlike the North Atlantic, the North Pacific has no region of deep-water formation so that internal fluctuations of the thermohaline circulation are not likely to be a source of low-frequency (decadal-interdecadal) climate variability there. Nevertheless, it is yet to be understood what effects (if any) low-frequency variability in convection and intermediate water production in the Sea of Okhotsk may have on the climate of the North Pacific. As pointed out by Hasselmann (1976), even a passive ocean, with its much higher heat capacity than the atmosphere, could integrate high-frequency atmospheric noise to produce a red response with variability at much lower frequencies. Such a response was indeed demonstrated in the model simulations of Hansen & Lebedeff (1987),

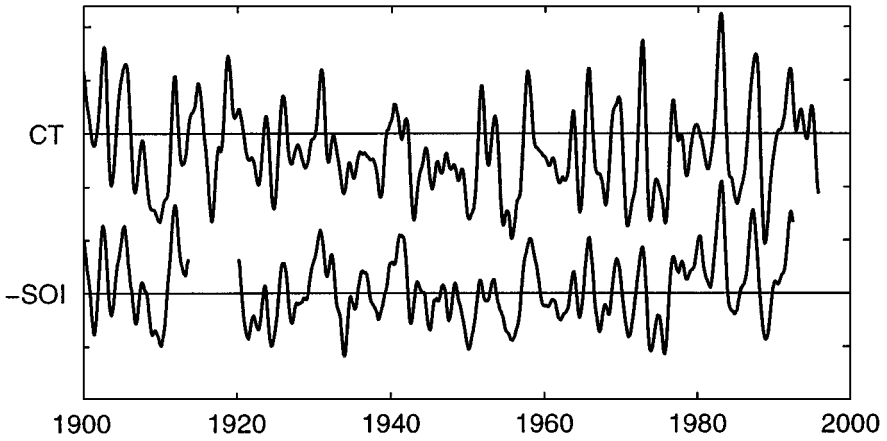

Figure 17 Cold tongue (CT) index based on SST in the equatorial Pacific (6°S–6°N, 180°W–90°W) and the Southern Oscillation Index (SOI) from pressure differences between stations at Darwin, Australia, and Tahiti with the sign reversed. Both time series have been smoothed with successive nine-month and five-month running mean filters. The interval between tick marks on the vertical axis is 1.0 standard deviation. These indices were kindly provided by Y Zhang & N Mantua.

where low-frequency climate variability was observed in a 100-year integration of the Goddard Institute for Space Studies atmospheric GCM coupled to a mixed layer ocean with specified ocean heat transport.

A number of theories exist to explain the observed decadal variability (Figures 18*b*, 19*b*) in the North Pacific. As seen in Figure 16, the Southern Oscillation Index (SLP anomalies at Tahiti minus Darwin, a statistical measure of ENSO) indicates that ENSO varies on decadal-interdecadal timescales (e.g. Trenberth 1990, Zhang et al 1997). Because ENSO is a nonlinear coupled tropical atmosphere-ocean phenomenon, it is possible that its decadal modulation and subsequent teleconnection to the North Pacific could explain the low-frequency variability observed there (Trenberth & Hurrel 1994). In this same area it may not be necessary to invoke a local nonlinearity of ENSO in the tropics. As pointed out by Gu & Philander (1997), a delayed negative feedback can be achieved through extratropical oceanic subduction of thermal anomalies (generated through the atmospheric teleconnection response to tropical SST anomalies) that slowly propagate along isopycnals toward the equator, where they reverse the sign of equatorial SSTs. Finally, Latif & Barnett (1994, 1996) have suggested a mode of decadal-interdecadal North Pacific variability solely involving midlatitude coupled atmosphere-ocean interactions and the strength of the subpolar gyre and its associated northward heat transport. As pointed

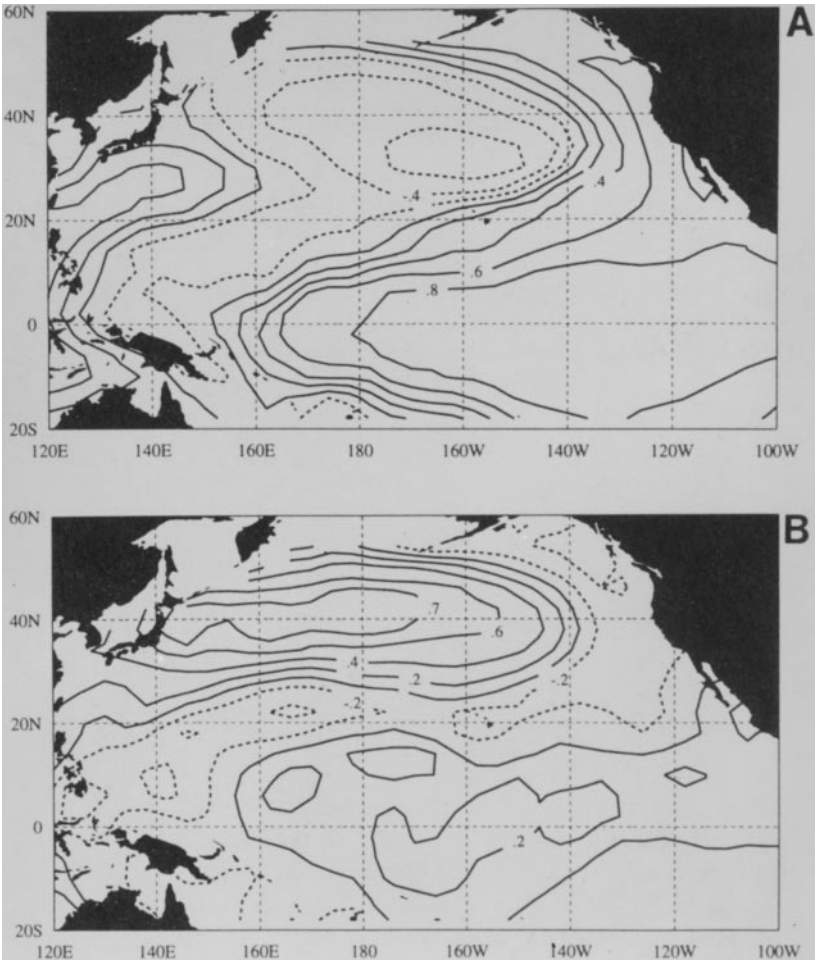

Figure 18 (*a*) Normalized EOF 1 (the interannual signal) of Pacific SSTs based on winter (November through March) anomalies during the period 1950–1951 to 1991–1992. The contour interval is 0.2, and negative contours are dashed. (*b*) As in Figure 18*a* but for EOF 2 (the decadal signal). The 0.7 contour is also shown. (From Deser & Blackmon 1995.)

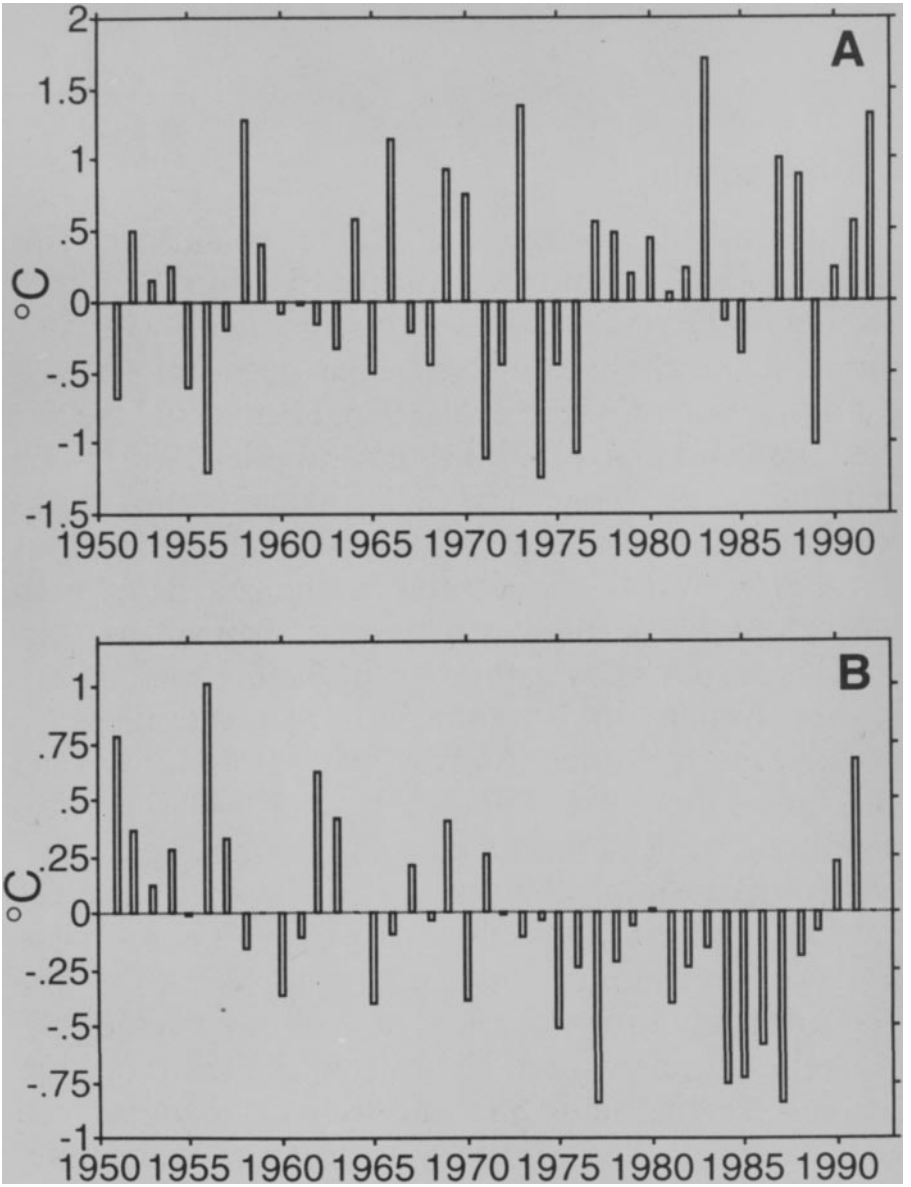

Figure 19 (*a*) Time series of SST anomalies averaged over the center of action of Figure 18*a*. (*b*) As in Figure 19*a* but for EOF 2 (Figure 18*b*) (From Deser & Blackmon 1995.)

out by Nakamura et al (1997), subtropical gyre SST variability on the decadal-interdecadal timescale is not solely explained through the tropical source, and some combination of the mechanisms may exist in reality. Below, these mechanisms and the evidence supporting them are discussed in more detail.

Figure 18 shows the first two EOFs of winter SST anomalies over the Pacific analyzed by Deser & Blackmon (1995). Similar structures have been identified by Kawamura (1994) and Zhang et al (1996, 1997). What is readily apparent is the distinctly different patterns expressed by the interannual (EOF 1) versus decadal (EOF 2) modes. The second EOF is primarily a North Pacific mode with maximum correlation centered on 40°N (the axis of the Kuroshio). It is also worth noting that the anomaly occurs as a linearly independent signal compared to tropical variability and is western intensified, perhaps indicative of gyre-scale as opposed to ENSO-modulated circulation changes (see Zhang et al 1996).

As shown by Deser & Blackmon (1995) and Zhang et al (1996), the preferential atmospheric teleconnection pattern associated with the North Pacific mode is similar to the well-known Pacific-North American (PNA) pattern (Wallace & Gutzler 1981). Trenberth & Hurrell (1994) devised a North Pacific index (NP) as the area-weighted mean SLP (November through March) over the region 30°–65°N, 160°E to 140°W. Figure 20*a* indicates the low-pass-filtered NP for the winter average, whereas Figure 20*b* indicates the spectrum for the time series 1924–1925 to 1990–1991. While not significant at the 95 percent level, there are several peaks in the two-to-six–year timescale (believed to be associated with ENSO), a deficit in power in the 7- to 12-year band, and a broad peak featuring timescales of 20 years and beyond.

The relationship between the North Pacific mode (Figures 18*b* and 19*b*) and the NP (Figure 20*a*) is readily apparent, with below normal values of the NP associated with below normal SST over the North Pacific (see also Trenberth & Hurrell 1994, their Figure 9). The main relationship is one in which changes in the atmospheric circulation are responsible for changes in the SST (e.g. Wallace et al 1990, Trenberth & Hurrell 1994, Deser & Blackmon 1995). Wind anomalies associated with the North Pacific index are maximum in the vicinity of the Aleutian low (Deser & Blackmon 1995), with stronger (weaker) westerlies associated with the cooler (warmer) SST. Along the west coast of North America the situation is reversed with below normal values of the NP associated with above normal SST due to the northward advection of warm waters on the eastern flank of the Aleutian low (Emery & Hamilton 1985).

While ENSO may modulate midlatitude thermal anomalies, a question arises as to how such anomalies persist through to the decadal timescale. Indeed, one would expect that thermal anomalies must ultimately be dissipated either

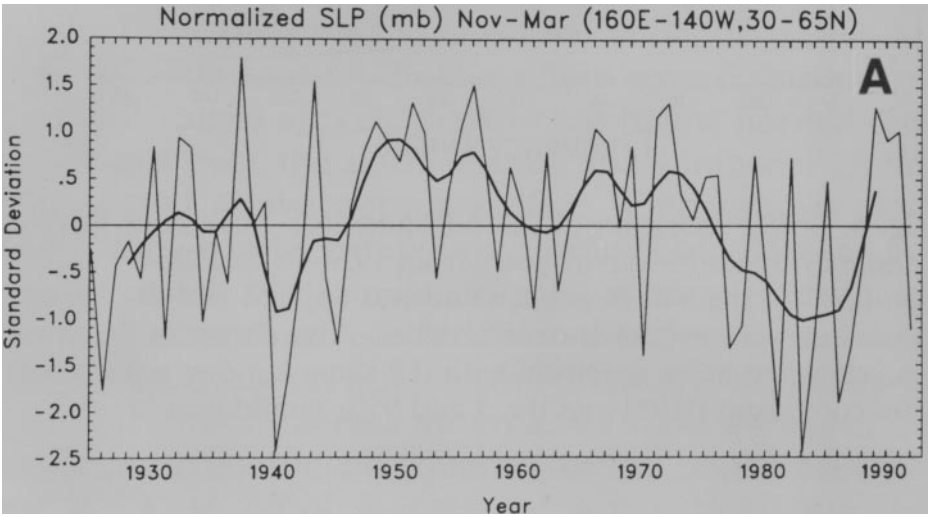

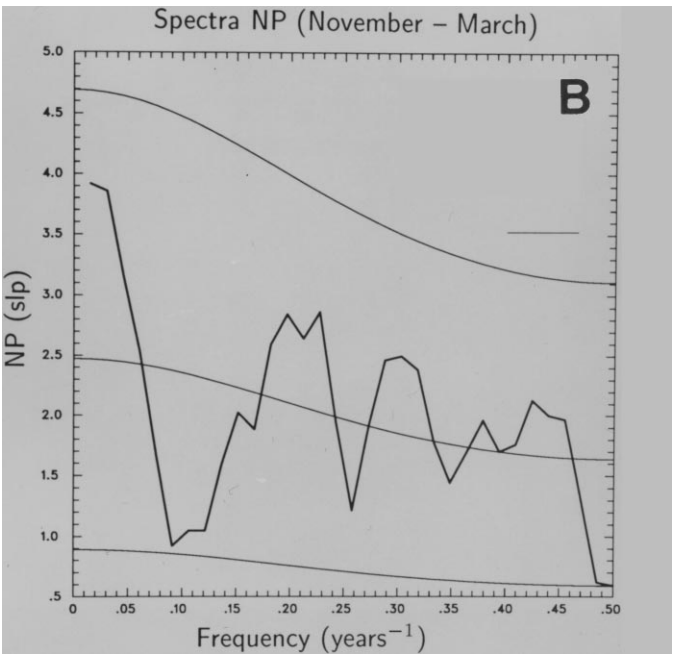

Figure 20 (*a*) Time series of the mean North Pacific SLPs for November–March. The total monthly mean value and the low-pass-filtered time series are shown. The filter employs seven weights (1, 4, 8, 10, 8, 4, 1)/ 36 across years to emphasize decadal time-scales. (*b*) Power spectrum of the NP index averages for the years 1924–1925 to 1990–1991. Also shown are the five and 95 percent confidence limits (*bottom and top smooth curves*), as well as the red noise spectrum (*middle smooth curve*) for the same lag one autocorrelation coefficient (0.91). (From Trenberth & Hurrell 1994.)

by ocean-atmosphere interaction (Alexander 1992*a*,1992*b*) (the most effective of which would be latent and sensible heat transfers) or by internal oceanic processes. Ocean surface anomalies created over the deep mixed layer in winter could be preserved below the summer thermocline and reappear at the surface during the following winter when the mixed layer deepens and intersects the anomaly (e.g. Namais & Born 1974, Alexander & Deser 1995). Persistent atmospheric features, such as the anomalous reoccurrence of intense Aleutian lows over decadal timescales, reinforce and further inject thermal anomalies into the deep mixed layer. These anomalies then subduct into the main pycnocline, where they flow southward along isopycnals (Deser et al 1996). Such thermal anomalies may then be transported (as a coherent structure) to later reemerge and alter the tropical Pacific SSTs (Gu & Philander 1997). In this manner, ENSO variability (e.g. more frequent occurrences of warm phases than cold phases or vice versa) could yield a decadal-interdecadal signal in the extratropical Pacific temperature, which in turn could give rise to a modulation of ENSO on a similar time scale and explain major phase shifts seen in the climate record (e.g. Trenberth 1990, Hastrom & Michaelson 1994, Minobe 1997, Mantua et al 1997, Nakamura et al 1997). Of course, such a phenomenon is inherently irregular owing to the ongoing effects of ENSO and midlatitude air-sea interactions, and additional irregularity could be imposed due to high-frequency weather.

Large-scale changes in heat content and transport of the Kuroshio and its extension can inject significant warm anomalies into the upper layer of the North Pacific, which extend with depth through to the core of the jet. In a similar fashion, reduction in Kuroshio transport favors expansion of the Oyashio and hence injection of cold thermal anomalies into the midlatitude gyre region (e.g. see Nakamura et al 1997, their Figure 1). Latif & Barnett (1994, 1996) (see also Latif 1998) describe the interdecadal vacillation as a gyre mode driven by midlatitude air-sea interactions without appealing to ENSO initiation or modification. Their coupled atmosphere-ocean modeling analysis suggested that this mode involved the weakening and strengthening of the subtropical gyre, which, through changes in heat transport in the western boundary through to the Kuroshio extension, creates SST anomalies in the central North Pacific (e.g. a strong gyre transports more heat into the central North Pacific via the Kuroshio extension, creating warm SST anomalies). A rather fascinating result was the subsequent strong atmospheric response to the central North Pacific SST anomalies in the PNA pattern, which acted locally to reinforce the anomalies. Changes in wind stress curl and the subsequent westward propagation of this signal in the ocean (via Rossby wave dynamics) then acted to spin down the subtropical gyre with the oscillation then entering the opposite phase. Support for the existence of such a mechanism in the observational record is given

by Zhang & Levitus (1997), where they found subsurface thermal anomalies circulating clockwise around the subtropical gyre, as in the work by Latif & Barnett (1994, 1996). Jin (1997) also developed a simple conceptual model involving the central dynamics discussed above and arrived at a delayed-oscillator model which also captured the essence of this variability.

As an alternative hypothesis, Jacobs et al (1994) argue that the 1982–1983 El Niño spawned such intense poleward traveling Kelvin waves, and subsequently westward radiated Rossby waves, that it ultimately displaced the Kuroshio axis northward, giving rise to a warm anomaly extending across the Pacific basin (see also McPhaden 1994). The anomaly (which extended from Japan to the west coast of North America) then persisted over an 11-year period. Although they use satellite observations to provide support for their model results, a number of questions arise. Although Kelvin waves can communicate equatorial signals poleward, the Rossby radius of deformation diminishes rapidly along the coast and isopycnals begin outcropping. By the time these Kelvin waves reach midlatitudes they have little energy available. Furthermore, coastal waters are heavily stratified (due to freshwater input by rivers) so that anomalies are trapped at the surface and therefore subject to degradation by surface heat loss. Finally, the model of Jacobs et al (1994) used observed wind stress data over the period 1981 to 1993, which implicitly contained the PNA teleconnection signal in it. It is therefore more likely that the Rossby wave response seen in their model arose from the oceanic adjustment to atmospheric wind perturbations rather than through communication via the coastal wave guide.

SUMMARY

In this review we have attempted to describe the important differences between the thermohaline circulation in the North Atlantic and Pacific Oceans. Our emphasis throughout this review was the interaction between these regions and the Arctic climate system. We took this perspective because the role of the Arctic in climate change and variability is often overlooked. Rather than simply describing the annual mean climatology and fundamental physical processes of the thermohaline circulation, we also focused on decadal-interdecadal climate variability in the high-latitude regions and the role of the ocean in this variability.

The single most important problem in determining the underlying physical mechanisms to explain (and ultimately to predict) the observed variability in the high-latitude North Atlantic and Pacific is the lack of an adequate observational network. Many of the historical data records are too short in time and too sparse in space to provide conclusive validation of proposed mechanisms for variability

on the decadal-interdecadal time scale. Consequently, further modeling studies in conjunction with and constrained by the observations must ultimately be carried out to unravel the underlying mechanisms.

One of the fundamental questions in the debate on climate change concerns the role of the oceans. By appealing to the results from both coupled atmosphere-ocean and atmosphere–mixed-layer ocean models we can begin to understand the differences between the North Atlantic and Pacific Ocean responses to increasing anthropogenic greenhouse gases. In the near term the ocean, through its large heat capacity, acts to reduce the effects of global warming relative to land. This is particularly noticeable in the high-latitude regions of the North Atlantic where a weakening of the thermohaline circulation and subsequent reduction in northward heat transport occurs. Both fully coupled atmosphere-ocean models (e.g. Gates et al 1992, Kattenberg et al 1996) and atmospheric models with only an ocean mixed layer (e.g. Mitchell et al 1990, Gates et al 1992) give similar responses in the Pacific Ocean, where there is a less active thermohaline circulation. Both classes of models further suggest that enhanced high-latitude warming is due to the reduction of sea ice cover and the accompanying decrease in surface albedo. Thus the Arctic is a prime location to look for a signal of anthropogenic climate change above the background natural climate variability.

Evidence for SAT changes over the Arctic Ocean is, however, inconsistent: Martin et al (1997) found significant warming in May and June from 1961 to 1990, whereas Kahl et al (1993) found cooling during autumn and winter over the western Arctic Ocean for 1950–1990. Trends in SAT over land are more apparent, as Chapman & Walsh (1993) report a significant increase over northwestern North America and central Siberia since 1960. A decrease in the Northern Hemisphere sea ice extent of about three percent per decade has also been observed (Chapman & Walsh 1993, Maslanik et al 1996, Cavalieri et al 1997).

Although it is apparent that we are only at the early stages of attempting to detect climate change at high latitudes and attributing this to anthropogenic effects, much progress will likely come in the near future. Of utmost importance is a deeper understanding of the mechanisms and structure of climate variability, as this is central to the detection and attribution issue. In addition, it is still unknown how the observed climate variability depends on the mean climatic state itself.

ACKNOWLEDGMENTS

This work was supported by NSERC strategic, operating, and Steacie Supplement grants, the Atmospheric Environments Service, the Canadian Institute for Climate Studies; and the NOAA Scripps Lamont Consortium on the Ocean's Role in Climate.

Literature Cited

Aagaard K, Carmack EC. 1989. The role of sea ice and other fresh water in the Arctic circulation. *J. Geophys. Res.* 94:14485–98

Aagaard K, Foldvik A, Hillman SR. 1987. The West Spitsbergen Current: disposition and water mass transformation. *J. Geophys. Res.* 92:3778–84

Aagaard K, Roach AT, Schumacher JD. 1985a. On the wind-driven variability of the flow through Bering Strait. *J. Geophys. Res.* 90: 7213–21

Aagaard K, Swift JH, Carmack EC. 1985b. Thermohaline circulation in the Arctic Mediterranean seas. *J. Geophys. Res.* 90:4833–46

Alexander MA. 1992a. Midlatitude atmosphere-ocean interaction during El Niño: Part I. the North Pacific Ocean. *J. Clim.* 5:944–58

Alexander MA. 1992b. Midlatitude atmosphere-ocean interaction during El Niño: Part II. the northern hemisphere atmosphere. *J. Clim.* 5:959–72

Alexander MA, Deser C. 1995. A mechanism for the recurrence of wintertime midlatitude SST anomalies. *J. Phys. Oceanogr.* 25:122–37

Anderson DLT, Willebrand J, eds. 1996. *Decadal Climate Variability: Dynamics and Predictability. NATO ASI Ser. I, Global Environ. Change*, Vol. 44. Berlin/New York: Springer-Verlag. 483 pp.

Armi L, Farmer DM. 1988. The flow of Mediterranean water through the Strait of Gibraltar. *Prog. Oceanogr.* 21:1–105

Barnston AG, Livezey RE. 1987. Classification, seasonality and persistence of low-frequency atmospheric circulation patterns. *Mon. Weather Rev.* 115:1083–126

Baumgartner A, Reichel E. 1975. *The World Water Balance*. Amsterdam/Lausanne/NY: Elsevier. 179 pp.

Berger WH. 1987. Ocean ventilation during the last 12,000 years: hypothesis of counterpoint deep water production. *Mar. Geol.* 78:1–10

Bjerknes J. 1964. Atlantic air-sea interaction. *Mon. Weather Rev.* 97:163–72

Bjerknes J. 1969. Atmospheric teleconnections from the equatorial Pacific. *Adv. Geophys.* 10:1–82

Borenäs KM, Lundberg PA. 1988. On the deep water flow through the Faroe Bank Channel. *J. Geophys. Res.* 93:1281–92

Boyd TJ, D'Asaro EA. 1994. Cooling of the West Spitsbergen Current: wintertime observations west of Svalbard. *J. Geophys. Res.* 99:22,597–618

Boyle EA. 1990. Quaternary deepwater paleoceanography. *Science* 249:863–70

Bretherton FP. 1982. Ocean climate modelling. *Prog. Oceanogr.* 11:93–129

Broecker WS. 1991. The great ocean conveyor. *Oceanography* 4:79–89

Broecker WS, Denton GH. 1989. The role of ocean-atmosphere reorganizations in glacial cycles. *Geochim. Cosmochim. Acta* 53:2465–501

Broecker WS, Peng TH, Jouzel J, Russel G. 1990. The magnitude of global fresh-water transports of importance to ocean circulation. *Clim. Dyn.* 4:73–79

Broecker WS, Peteet DM, Rind D. 1985. Does the ocean-atmosphere system have more than one stable mode of operation? *Nature* 315: 21–26

Bryden HL, Roemmich DH, Church JA. 1991. Ocean heat transport across 24 N in the Pacific. *Deep-Sea Res.* 38:297–324

Buorke RH, Weigel AM, Paquette RG. 1988. The westward turning branch of the West Spitsbergen Current. *J. Geophys. Res.* 93:14,065–77

Carmack EC. 1990. Large scale physical oceanography of Polar oceans. In *Polar Oceanography, Part A: Physical Science*, ed. WM Smith Jr., p. 171–222. New York: Academic. 406 pp.

Carmack EC, Aagaard K, Swift JH, MacDonald RW, McLaughlin FA, et al. 1998. Changes in temperature and tracer distributions within the Arctic Ocean: results from the 1994 Arctic Ocean section. *Deep-Sea Res.* 44:1487–502

Carmack EC, Macdonald RW, Perkin RG, McLaughlin FA, Pearson RJ. 1995. Evidence for warming of Atlantic water in the southern Canadian Basin of the Arctic Ocean: results from the Larsen-93 expedition. *Geophys. Res. Lett.* 22:1061–64

Cattle H. 1985. Diverting Soviet rivers: some possible repercussions for the Arctic Ocean. *Polar Rec.* 22:485–98

Cavalieri D, Gloersen JP, Parkinson CL, Comiso JC, Zwally HJ. 1997. Observed hemispheric asymmetry in global sea ice changes. *Science* 278:1104–06

Chapman WL, Walsh JE. 1993. Recent variations of sea ice and air temperature in high latitudes. *Bull. Am. Meteorol. Soc.* 74:33–47

Clarke RA. 1984. Transport through the Cape-Farewell-Flemish Cap section. *Rapp. Reun. Cons. Int. Explor. Mer.* 185:120–30

Coachman LK, Aagaard K. 1988. Transports through Bering Strait: annual and interannual variability. *J. Geophys. Res.* 93:15,535–39

Curry WB, Duplessy JC, Labeyrie LD, Shackleton NJ. 1988. Changes in the distribution of $\delta^{13}C$ of deep water ΣCO_2 between the last glaciation and the Holocene. *Paleoceanography* 3:317–41

Dean WE, Gardner JV, Hemphill-Halet E. 1989. Changes in redox conditions in deep-sea sediments of the sub-Arctic North Pacific Ocean: possible evidence for the presence of North Pacific Deep Water. *Paleoceanography* 4:639–53

Delworth T, Manabe S, Stouffer RJ. 1993. Interdecadal variations of the thermohaline circulation in a coupled ocean-atmosphere model. *J. Clim.* 6:1993–2011

Delworth T, Manabe S, Stouffer RJ. 1997. Multidecadal climate variability in the Greenland sea and surrounding regions: a coupled model simulation. *Geophys. Res. Lett.* 24:257–60

Deser C, Alexander MA, Timlin MS. 1996. Upper-ocean thermal variations in the North Pacific during 1970–1991. *J. Clim.* 9:1840–55

Deser C, Blackmon ML. 1993. Surface climate variations over the North Atlantic Ocean during winter: 1900–1989. *J. Clim.* 6:1743–53

Deser C, Blackmon ML. 1995. On the relationship between tropical and North Pacific sea surface temperature variations. *J. Clim.* 8:1677–80

Dettinger MD, Cayan DR. 1995. Large-scale atmospheric forcing of recent trends toward early snowmelt runoff in California. *J. Clim.* 8:606–23

Dickson RR, Brown J. 1994. The production of North Atlantic Deep Water: sources, sinks and pathways. *J. Geophys. Res.* 99:12,319–41

Dickson RR, Gmitrowicz EM, Watson AJ. 1990. Deep-water renewal in the northern North Atlantic. *Nature* 344:848–50

Dickson RR, Lazier J, Meincke J, Rhines P, Swift J. 1996. Long-term coordinated changes in the convective activity of the North Atlantic. *Prog. Oceanogr.* 38:205–39

Dickson RR, Meincke J, Malmberg SA, Lee AJ. 1988. The "great salinity anomaly" in the northern North Atlantic 1968–1982. *Prog. Oceanogr.* 20:103–51

Duplessy JC, Shackleton NJ, Fairbanks RG, Labeyrie L, Oppo D, Kallel N. 1988. Deep-water source variations during the last climate cycle and their impact on the global deep-water circulation. *Paleoceanography* 3:343–60

Ellis GE. 1868. *Memoir of Sir Benjamin Thompson, Count Rumford, with Notices from his Daughter*. Am. Acad. Sci. Philadelphia, PA: Claxton, Remsen Haffelfinger

Ellis H. 1751. A Letter to the Rev. Dr. Hales, F.R.S. from Captain Henry Ellis, F.R.S. dated Jan. 7, 1750–51, at Cape Monte Africa, Ship Earl of Halifax. *Philos. Trans. R. Soc. London* 47:211–14

Emery WJ, Hamilton K. 1985. Atmospheric forcing of interannual variability in the northeast Pacific Ocean: connections with El Niño. *J. Geophys. Res.* 90:857–68

Fang Z, Wallace JM. 1994. Arctic sea ice variability on a timescale of weeks and its relation to atmospheric forcing. J. Clim. 7:1897–913

Fissel DB, Loemon DD, Melling H, Lake RA. 1988. Non-tidal flows in the Northwest Passage. *Can. Tech. Rep. Hydrogr. Ocean Sci. 98*, Sidney, BC: Inst. Ocean Sci.

Foldvik A, Gammelsrød T. 1988. Notes on Southern Ocean hydrography, sea-ice and bottom water formation. *Palaeogeogr. Palaeoclimatol. Palaeoecol.* 67:3–17

Ganopolski A, Rahmstorf S, Petoukhov V, Claussen M. 1998. Simulation of modern and glacial climates with a coupled global model of intermediate complexity. *Nature* 391:351–56

Gates WL, Mitchell JFB, Boer GJ, Cubasch U, Meleshko VP. 1992. Climate modelling, climate prediction and model validation. In *Climate Change 1992, the Supplementary Report to the IPCC Scientific Assessment*, ed. JT Houghton, BA Callander, SK Varney, p. 97–134. New York/London: Cambridge Univ. Press. 200 pp.

Gerdes R, Schauer U. 1997. Large-scale circulation and water mass distribution in the Arctic Ocean from model results and observations. *J. Geophys. Res.* 102:8467–83

Gordon AL. 1986. Interocean exchange of intermediate water. *J. Geophys. Res.* 91:5037-46

Grumbine RW. 1991. A model of the formation of high-salinity shelf water on polar continental shelves. *J. Geophys. Res.* 96:22,049–62

Gu D, Philander GH. 1997. Internal climate fluctuations that depend on exchanges between the tropics and extratropics. *Science* 275:805–7

Häkkinen S. 1993. An Arctic source for the Great Salinity Anomaly: a simulation of the Arctic ice-ocean system for 1955–1975. *J. Geophys. Res.* 98:16,397–410

Hall MM, Bryden HL. 1982. Direct estimates and mechanisms of ocean heat transport. *Deep-Sea Res.* 29:339–59

Hallock ZR, Teague WJ. 1996. Evidence for a North Pacific deep western boundary current. *J. Geophys. Res.* 101:6617–24

Hansen DV, Bezdek H. 1996. On the nature of

decadal anomalies in North Atlantic sea surface temperature. *J. Geophys. Res.* 101:8749–58

Hansen J, Lebedeff S. 1987. Global trends of measured surface air temperature. *J. Geophys. Res.* 92:13,345–72

Hasselmann K. 1976. Stochastic climate models: Part I. theory. *Tellus* 28:239–305

Hastrom L, Michaelson J. 1994. Long-term central coastal California precipitation variability and relationships to El Niño. *J. Clim.* 7:1373–87

Hasunuma K. 1978. Formation of the intermediate salinity minimum in the northwestern Pacific Ocean. *Bull. Ocean Res. Inst.* 9. 47 pp.

Holland WR. 1973. Baroclinic and topographic influences on the transport in western boundary currents. *Geophys. Fluid Dyn.* 4:187–210

Horel JD, Wallace JM. 1981. Planetary-scale atmospheric phenomena associated with the Southern Oscillation. *Mon. Weather Rev.* 109:813–29

Hughes TMC, Weaver AJ. 1994. Multiple equilibria in an asymmetric two-basin ocean model. *J. Phys. Oceanogr.* 24:619–37

Hurrell JW. 1995. Decadal trends in the North Atlantic Oscillation: regional temperatures and precipitation. *Science* 269:676–79

Hurrell JW. 1996. Influence of variations in extratropical wintertime teleconnections on Northern Hemisphere temperature. *Geophys. Res. Lett.* 23:665–68

Ivers WD. 1975. The deep circulation of the North Atlantic with especial reference to the Labrador Sea. PhD thesis. Univ. Calif., San Diego. 179 pp.

Jacobs GA, Hurlburt HE, Kindle JC, Metzger EJ, Mitchell JL, et al. 1994. Decade-scale trans-Pacific propagation and warming effects of an El Niño warming. *Nature* 370:360–63

Jacobs SS, Fairbanks RG, Horibe Y. 1985. Origin and evolution of water masses near the Antarctic continental margin: evidence from $H_2{}^{18}O/H_2{}^{16}O$ ratios in seawater. In *Oceanology of the Antarctic Continental Shelf, Antarct. Res. Ser.*, Vol. 43. ed. SS Jacobs, p. 58–86. Washington, DC: AGU

Jin F. 1997. A theory of interdecadal climate variability of the North Pacific ocean-atmosphere system. *J. Clim.* 10:1821–35

Johnson GC. 1990. *Near-equatorial deep circulation in the Indian and Pacific Oceans*. PhD thesis. Woods Hole, MA: Woods Hole Oceanogr. Inst.

Johnson GC, Toole JM. 1993. Flow of deep and bottom waters in the Pacific at 10°N. *Deep-Sea Res.* 40:371–94

Joyce TM, Warren BA, Talley LD. 1986. The geothermal heating of the abyssal subarctic Pacific Ocean. *Deep-Sea Res.* 33:1003–15

Kahl JK, Charlevoix DJ, Zaitseva NA, Schnell RC, Serreze MC. 1993. Absence of evidence for greenhouse warming over the Arctic Ocean in the past 40 years. *Nature* 361:335–37

Kattenberg A, Giorgi F, Grassl H, Meehl GA, Mitchell JFB, et al. 1996. Climate models—projections of future climate. In *Climate Change 1995, the Science of Climate Change*, ed. JT Houghton, LG Meira Filho, BA Callander, N Harris, A Kattenberg, K Maskell, p. 285–357. New York/London: Cambridge Univ. Press. 572 pp.

Kawamura R. 1994. A rotated EOF analysis of global sea surface temperature variability with interannual and interdecadal scales, *J. Phys. Oceanogr.* 24:707–15

Kawase M. 1987. Establishment of deep ocean circulation driven by deep-water production. *J. Phys. Oceanogr.* 17:2294–317

Keigwin LD. 1987. North Pacific deep water formation during the latest glaciation. *Nature* 330:362–64

Killworth PD. 1979. On "chimney" formations in the ocean. *J. Phys. Oceanogr.* 9:531–54

Killworth PD. 1983. Deep convection in the world ocean. *Rev. Geophys. Space Phys.* 21:1–26

Kirwan R. 1787. *An Estimate of Temperature at Different Latitudes*. London.

Krauss W. 1986. The North Atlantic Current. *J. Geophys. Res.* 91:5061–74

Kuo HH, Veronis G. 1973. The use of oxygen as a test for an abyssal circulation model. *Deep-Sea Res.* 20:871–88

Kushnir Y. 1994. Interdecadal variability in the Northern Hemisphere sea surface temperature and associated atmospheric conditions. *J. Clim.* 7:141–57

Kushnir Y, Held IM. 1997. Equilibrium atmospheric response to North Atlantic SST anomalies. *J. Clim.* 9:1208–20

Kushnir Y, Lau NC. 1992. The general circulation model response to a North Pacific SST anomaly: dependence on timescale and pattern polarity. *J. Clim.* 5:271–83

Latif M. 1998. Dynamics of interdecadal variability in coupled ocean-atmosphere models. *J. Clim.* 11:602–24

Latif M, Barnett TP. 1994. Causes of decadal climate variability over the North Pacific and North America. *Science* 266:634–37

Latif M, Barnett TP. 1996. Decadal climate variability over the North Pacific and North America: dynamics and predictability. *J. Clim.* 9:2407–23

Lau NC, Nath MJ. 1994. A modeling study of the relative roles of tropical and extratropical SST anomalies in the variability of the global atmosphere-ocean system. *J. Clim.* 7:1184–207

Lazier JRN. 1980. Oceanographic conditions at Ocean Weather Ship *Bravo*, 1964–1974. *Atmos-Ocean* 18:227–38

Leaman DK, Schott FA. 1991. Hydrographic structure of the convective regime of the Gulf of Lions: winter 1987. *J. Phys. Oceanogr.* 21: 575–98

Lee TN, Johns WE, Zantopp RJ, Fillenbaum ER. 1996. Moored observations of western boundary current variability and thermohaline circulation at 26.5°N in the subtropical North Atlantic. *J. Phys. Oceanogr.* 26:962–83

Manabe S, Stouffer RJ. 1998. Two stable equilibria of a coupled ocean-atmosphere model. *J. Clim.* 1:841–66

Manley TO. 1995. Branching of Atlantic water within the Greenland-Spitsbergen passage: an estimate of recirculation. *J. Geophys. Res.* 100:20,627–34

Mantua NJ, Hare SR, Zhang Y, Wallace JM, Francis RC. 1997. A Pacific interdecadal climate oscillation with impacts on salmon production. *Bull. Am. Meteorol. Soc.* 78:1069–79

Mantyla AW, Reid JL. 1983. Abyssal characteristics of the world ocean waters. *Deep-Sea Res.* 30:805–33

Martin S, Munoz E. 1997. Properties of the Arctic 2-meter air temperature for 1979–present derived from a new gridded data set. *J. Clim.* 10:1428–40

Martin S, Munoz E, Drucker R. 1997. Recent observations of spring-summer surface warming over the Arctic Ocean. *Geophys. Res. Lett.* 24:1259–62

Maslanik JA, Serreze MC, Barry RG. 1996. Recent decrease in Arctic summer ice cover and linkages to atmospheric circulation anomalies. *Geophys. Res. Lett.* 23:1677–80

Mauritzen C, Häkkinen S. 1997. Influence of sea ice on the thermohaline circulation in the Arctic-North Atlantic Ocean. *Geophys. Res. Lett.* 24:3257–60

Maykut GA. 1982. Large-scale heat exchange and ice production in the central Arctic. *J. Geophys. Res.* 87:7971–84

McCartney MS. 1992. Recirculating components to the deep boundary current of the northern North Atlantic. *Prog. Oceanogr.* 29: 283–383

McCartney MS, Bennett SL, Woodgate-Jones ME. 1991. Eastward flow through the Mid-Atlantic Ridge at 11°N and its influence on the abyss of the eastern basin. *J. Phys. Oceanogr.* 21:1089–121

McCartney MS, Talley LD. 1984. Warm-to-cold water conversion in the northern North Atlantic Ocean. *J. Phys. Oceanogr.* 14:922–35

McLaughlin FA, Carmack EC, Mcdonald RW, Bishop JKB. 1996. Physical and geochemical properties across the Atlantic/Pacific water mass front in the southern Canadian Basin. *J. Geophys. Res.* 101:1183–97

McPhaden M. 1994. The eleven year El Niño? *Nature* 370:326–27

Meincke J. 1983. The modern current regime across the Greenland-Scotland ridge. In *Structure and Development of the Greenland-Scotland Ridge*, ed. A Bott et al, p. 637–650, London/New York: Plenum

Minobe S. 1997. A 50–70 year climatic oscillation over the North Pacific and North America. *Geophys. Res. Lett.* 24:683–86

Mitchell JFB, Manabe S, Meleshko V, Tokioka T. 1990. Equilibrium climate change and its implications for the future. In *Climate Change The IPCC Scientific Assessment*, ed. JT Houghton, GJ Jenkins, JJ Ephraums, p. 131–172. New York/London: Cambridge Univ. Press. 365 pp.

Morison J. 1991. Seasonal variations in the West Spitsbergen Current estimated from bottom pressure measurements. *J. Geophys. Res.* 96:18381–95

Mysak LA. 1986. El Niño, interannual variability and the fisheries in the northeast Pacific Ocean. *Can. J. Fish. Aquat. Sci.* 43:464–97

Mysak LA, Manak DK. 1989. Arctic sea-ice extent and anomalies, 1953–1984. *Atmos. Ocean* 27:376–405

Mysak LA, Manak DK, Marsden RF. 1990. Sea-ice anomalies observed in the Greenland and Labrador Seas during 1901–1984 and their relation to an interdecadal Arctic climate cycle. *Clim. Dyn.* 5:111–33

Nakamura H, Lin G, Yamagata T. 1997. Decadal climate variability in the North Pacific during the recent decades. *Bull. Am. Meteorol. Soc.* 78:2215–25

Nakamura N, Oort AH. 1988. Atmospheric heat budgets of the polar regions. *J. Geophys. Res.* 93:9510–24

Namais J, Born RM. 1974. Further studies of temporal coherence in North Pacific sea surface temperatures. *J. Geophys. Res.* 79:797–98

Nitta T, Yamada S. 1989. Recent warming of tropical sea surface temperature and its relationship to the Northern Hemisphere circulation. *J. Meteorol. Soc. Jpn.* 67:187–93

Oort AH. 1974. Year-to-year variations in the energy balance of the Arctic atmosphere. *J. Geophys. Res.* 79:1253–60

Oppo DW, Fairbanks RG. 1990. Atlantic thermohaline circulation of the last 150,000 years: relationship to climate and atmospheric CO_2. *Paleoceanography* 5:277–88

Overland JE, Pease CH. 1982. Cyclone climatology of the Bering Sea and its relation to sea ice extent. *Mon. Weather Rev.* 110:5–13

Overland JE, Roach AT. 1987. Northward flow in the Bering and Chukchi Seas. *J. Geophys. Res.* 92:7097–105

Overland JE, Turet P. 1994. Variability of the atmospheric energy flux across 70°N computed from the GFDL data set. In *Polar Oceans and Their Role in Shaping the Global Environment, Geophys. Monogr. Ser.*, Vol. 85. ed. OM Johannessen, RD Muench JE Overland, p. 313–25. Washington, DC: AGU

Overland JE, Turet P, Oort AH. 1996. Regional variations of the moist static energy flux into the Arctic. *J. Clim.* 9:54–65

Palmer TN, Sun Z. 1985. A modeling and observational study of the relationship between sea surface temperatures in the northwest Atlantic and the atmospheric general circulation. *Q. J. R. Meteorol. Soc.* 111:947–75

Peng S, Mysak LA, Ritchie H, Derome J, Dugas B. 1995. The differences between early and midwinter atmospheric responses to sea surface temperature anomalies in the northwest Atlantic. *J. Clim.* 8:137–57

Peng S, Robinson WA, Hoerling MP. 1997. The modeled atmospheric response to midlatitude SST anomalies and its dependence on background circulation states. *J. Clim.* 10:971–87

Pitcher EJ, Blackmon ML, Bates GT, Munoz S. 1988. The effect of North Pacific sea surface temperature anomalies on the January climate of a general circulation model. *J. Atmos. Sci.* 45:226–46

Price JF, Baringer MO. 1994. Outflows and deep water production by marginal seas. *Prog. Oceanogr.* 33:161–200

Quadfasel D, Gascard JC, Koltermann KP. 1987. Large-scale oceanography in Fram Strait during the 1984 Marginal Ice Zone Experiment. *J. Geophys. Res.* 92:6719–28

Rahmstorf S. 1995. Bifurcations of the Atlantic thermohaline circulation in response to changes in the hydrological cycle. *Nature* 378:145–49

Reid JL. 1961. On the temperature, salinity and density differences between the Atlantic and Pacific Oceans in the upper kilometre. *Deep-Sea Res.* 7:265–75

Reid JL. 1979. On the contribution of Mediterranean Sea outflow to the Norwegian-Greenland Sea. *Deep-Sea Res.* 26:1199–223

Reid JL. 1997. On the total geostrophic circulation of the Pacific Ocean: flow patterns, tracers and transports. *Prog. Oceanogr.* 39:263–352

Reverdin G, Cayan D, Kushnir Y. 1997. Decadal variability of hydrography in the upper northern North Atlantic in 1948–1990. *J. Geophys. Res.* 102:8505–31

Rhein M. 1991. Ventilation rates of the Greenland and Norwegian Seas derived from the distributions of chlorofluoromethanes F11 and F12, *Deep-Sea Res.* 38:485–503

Rintoul SR. 1991. South Atlantic interbasin exchange. *J. Geophys. Res.* 96:2675–92

Roach AT, Aagaard K, Pease CH, Salo SA, Weingartner T, Pavlov V, Kulakov M. 1995. Direct measurements of transport and water properties through the Bering Strait. *J. Geophys. Res.* 100:18,443–57

Roemmich DH, Wunsch C. 1985. Two transatlantic sections: meridional circulation and heat flux in the subtropical North Atlantic Ocean. *Deep-Sea Res.* 32:619–64

Rogers JC. 1981. North Pacific Oscillation. *J. Climatol.* 1:39–57

Rogers JC. 1990. Patterns of low-frequency monthly sea level pressure variability (1988–1986) and associate wave cyclone frequency. *J. Clim.* 3:1364–79

Rogers JC, van Loon H. 1979. The seesaw in winter temperatures between Greenland and northern Europe: Part II. some oceanic and atmospheric effects in middle and high latitudes. *Mon. Weather Rev.* 107:509–19

Ross CK. 1984. Temperature-salinity characteristic of the 'overflow' water in Denmark Strait during "OVERFLOW 73," *Rapp. Reun. Cons. Int. Explor. Mer.* 185:111–19

Rudels B, Jones EP, Anderson LG, Kattner G. 1994. On the intermediate depth waters of the Arctic Ocean. In *The Polar Oceans and Their Role in Shaping the Global Environment, Geophys. Monogr. Ser.*, Vol. 85, ed. OM Johannessen, RD Muench JE Overland, p. 33–46. Washington, DC: AGU

Rudels B, Quadfasel D, Friedrich H. 1989. Greenland Sea convection in the winter of 1987–1988. *J. Geophys. Res.* 94:3223–27

Saunders PM. 1990. Cold outflow from the Faroe Bank Channel. *J. Phys. Oceanogr.* 20: 29–43

Saunders PM. 1994. The flux of overflow water through the Charlie-Gibbs Fracture Zone. *J. Geophys. Res.* 99:12,343–55

Saunders PM. 1996. The flux of dense cold overflow water southeast of Iceland. *J. Phys. Oceanogr.* 26:85–95

Schmitt RW, Bogden PS, Dorman CE. 1989. Evaporation minus precipitation and density fluxes for the North Atlantic. *J. Phys. Oceanogr.* 19:1208–21

Schmitz WJ Jr, 1995. On the interbasin-scale thermohaline circulation. *Rev. Geophys.* 33:151–73

Schmitz WJ Jr, McCartney MS. 1993. On the North Atlantic circulation. *Rev. Geophys.* 31:29–49

Schmitz WJ Jr, Richardson PL. 1991. On the sources of the Florida Current. *Deep-Sea Res.* 38, 1:S389–S409 (Suppl.)

Schmitz WJ Jr, Thompson JD, Luyten JR. 1992.

The Sverdrup circulation for the Atlantic along 24°N. *J. Geophys. Res.* 97:7251–56

Schott F, Visbeck M, Fischer J. 1993. Observations of vertical currents and convection in the central Greenland Sea during the winter of 1988–1989. *J. Geophys. Res.* 98:14,401–21

Serreze M, Barry R, McLaren AS. 1989. Seasonal variations in sea ice motion and effects on sea ice concentration in the Canadian Basin. *J. Geophys. Res.* 94:10,955–70

Serreze MC, Barry RG, Rehder MC, Walsh JE. 1995. Variability of atmospheric circulation and moisture flux over the Arctic. *Philos. Trans. R. Soc. London* 352:215–25

Serreze MC, Box JE, Barry RG, Walsh JE. 1993. Characteristics of Arctic synoptic activity, 1952–1989. *Meteorol. Atmos. Phys.* 51:147–64

Serreze M, Carse F, Barry R, Rogers JC. 1997. Icelandic low cyclone activity: climatological features, linkages with the NAO, and relationships with recent changes in the Northern Hemisphere circulation. *J. Clim.* 10:453–63

Shackleton NJ, Duplessy JC, Arnold M, Maurice P, Hall A, Cartlidge J. 1988. Radiocarbon age of last glacial Pacific deepwater. *Nature* 335:708–11

Shaffer G, Bendtsen J. 1994. Role of the Bering Strait in controlling North Atlantic Ocean circulation and climate. *Nature* 367:354–57

Siedler G. 1969. General circulation of water masses in the Red Sea. In *Hot Brines and Recent Heavy Metal Deposits in the Red Sea*, ed. ET Degen, DA Ross, p. 131–37. Berlin/New York: Springer-Verlag

Slonosky VC, Mysak LA, Derome J. 1997. Linking Arctic sea-ice and atmospheric circulation anomalies on interannual and decadal timescales. *Atmos. Ocean* 35:333–66

Steele M, Thomas D, Rothrock D, Martin S. 1996. A simple model study of the Arctic Ocean freshwater balance, 1979–1985. *J. Geophys. Res.* 101:20833–48

Stigebrandt A. 1984. The North Pacific: a global-scale estuary. *J. Phys. Oceanogr.* 14: 464–70

Stocker TF, Wright DG. 1991. Rapid transitions of the ocean's deep circulation induced by changes in surface water fluxes. *Nature* 351:729–32

Stocker TF, Wright DG, Mysak LA. 1992. A zonally averaged, coupled ocean-atmosphere model for paleoclimate studies. *J. Clim.* 5: 773–97

Stommel H. 1957. A survey of ocean current theory. *Deep-Sea Res.* 4:149–84

Stommel H, Árons AB. 1960. On the abyssal circulation of the world ocean: II. an idealized model of the circulation pattern and amplitude in ocean basins. *Deep-Sea Res.* 6:217–33

Swift JH, Aagaard K. 1981. Seasonal transitions and water mass formation in the Iceland and Greenland Seas. *Deep-Sea Res.* 28:1107–29

Swift JH, Jones EP, Aagaard K, Carmack EC, Hingston M, et al. 1998. Waters of the Makarov and Canada basins. *Deep-Sea Res.* 44:1503–29

Taft BA, Hayes SP, Frederich GE, Codispoti LA. 1991. Flow of abyssal water into Samoa Passage. *Deep-Sea Res.* 38, Suppl. 1: S103–28

Talley LD. 1991. An Okhotsk Sea water anomaly: implications for ventilation in the North Pacific. *Deep-Sea Res.* 38, Suppl. 1: S171–90

Talley LD. 1993. Distribution and formation of North Pacific Intermediate Water. *J. Phys. Oceanogr.* 23:517–37

Talley LD, McCartney MS. 1982. Distribution and circulation of Labrador Sea Water. *J. Phys. Oceanogr.* 12:1189–205

Talley LD, Nagata Y, Fujimura M, Iwao T, Kono T, et al. 1995. North Pacific Intermediate Water in the Kuroshio/Oyashio mixed water region. *J. Phys. Oceanogr.* 25:475–501

Thompson N, Count Rumford. 1798. The propagation of heat in fluids. Reproduced, 1870, In *The Complete Works of Count Rumford*. Vol. 1, p. 237–400. Boston, MA: Am. Acad. Sci.

Ting M. 1991. The stationary wave response to a midlatitude SST anomaly in an idealized GCM. *J. Atmos. Sci.* 48:1249–75

Trenberth KE. 1990. Recent observed interdecadal climate changes in the Northern Hemisphere. *Bull. Am. Meteorol. Soc.* 71:988–93

Trenberth KE, Hoar TJ. 1994. The 1990–1995 El Niño-Southern Oscillation event: longest on record. *Geophys. Res. Lett.* 23:57–60

Trenberth KE, Hurrell JW. 1994. Decadal atmosphere-ocean variations in the Pacific. *Clim. Dyn.* 9:303–19

van Loon H, Rogers JC. 1978. The seesaw in winter temperatures between Greenland and northern Europe: Part I. general description. *Mon. Weather Rev.* 106:296–310

Vowinckel E, Orvig S. 1971. Synoptic heat budgets at three polar stations. *J. Appl. Meteorol.* 10:387–96

Walker GT, Bliss EW. 1932. World weather V. *Mem. R. Meteorol. Soc.* 4:53–84

Wallace JM, Gutzler DS. 1981. Teleconnections in the geopotential height field during the Northern Hemisphere winter. *Mon. Weather Rev.* 109:784–812

Wallace JM, Jiang Q. 1987. On the observed structure of the interannual variability of the

atmosphere-ocean climate system. In *Atmospheric and Oceanic Variability*, ed. H Cattle, p. 17–43. London: R. Meteorol. Soc.
Wallace JM, Smith C, Jiang Q. 1990. Spatial patterns of atmosphere-ocean interaction in the northern winter. *J. Clim.* 3:990–98
Walsh JE, Chapman WL. 1990. Arctic contribution to upper-ocean variability in the North Atlantic. *J. Clim.* 3:1462–73
Walsh JE, Johnson CM. 1979. Interannual atmospheric variability and associated fluctuations in Arctic sea ice extent. *J. Geophys. Res.* 84:6915–28
Wang X, Stone P, Marotzke J. 1995. Poleward heat transport in a barotropic ocean model. *J. Phys. Oceanogr.* 25:256–65
Warren BA. 1973. Transpacific hydrographic sections at lats. 43°S and 28°S: the SCORPIO Expedition: II. deep water. *Deep-Sea Res.* 20:9–38
Warren BA. 1981. Deep circulation of the World Ocean. In *Evolution of Physical Oceanography*, ed. BA Warren, C Wunsch, p. 6–41. Cambridge, MA: MIT Press. 620 pp.
Warren BA. 1983. Why is no deep water formed in the North Pacific? *J. Mar. Res.* 41:327–47
Warren BA, Owens WB. 1988. Deep currents in the central subarctic Pacific Ocean. *J. Phys. Oceanogr.* 18:529–51
Watanabe T, Wakatsuchi M. 1998. Formation of 26.8–26.9 σ_θ water in the Kuril Basin of the Sea of Okhotsk as a possible origin of North Pacific Intermediate Water. *J. Geophys. Res.* 103:2849–65
Weare B, Navato A, Newell RE. 1976. Empirical orthogonal analysis of Pacific Ocean sea surface temperature. *J. Phys. Oceanogr.* 6:671–78
Weaver AJ, Eby M, Fanning AF, Wiebe EC. 1998. The climate of the Last Glacial Maximum in a coupled ocean GCM/energy-moisture balance atmosphere model. *Nature* 394:847–53
Weaver AJ, Marotzke J, Cummins PF, Sarachik ES. 1993. Stability and variability of the thermohaline circulation. *J. Phys. Oceanogr.* 23:39–60
Weaver AJ, Sarachik ES. 1991. Evidence for decadal variability in an ocean general circulation model: an advective mechanism. *Atmos.-Ocean* 29:197–231
Weaver AJ, Sarachik ES, Marotzke J. 1991. Freshwater flux forcing of decadal and interdecadal oceanic variability. *Nature* 353:836–38
Weaver AJ, Valcke S. 1998. On the variability of the thermohaline circulation in the GFDL coupled model. *J. Clim.* 11:759–67
Weyl PK. 1968. The role of the oceans in climatic change: a theory of the Ice Ages. *Meteorol. Monogr.* 8:37–62
Whittaker LM, Horn LH. 1984. Northern Hemisphere extratropical cyclone activity for four mid-season months. *J. Climatol.* 9:297–319
Wijffels SE, Schmitt RW, Bryden HL, Stigebrandt A. 1992. Transport of freshwater by the oceans. *J. Phys. Oceanogr.* 22:155–62
Wohlleben TMH, Weaver AJ. 1995. Interdecadal climate variability in the subpolar North Atlantic. *Clim. Dyn.* 11:459–67
Worthington LV. 1976. *On the North Atlantic Circulation. Oceanogr. Stud. 6, Baltimore, MD:* The Johns Hopkins Univ. 110 pp.
Wyrtki K. 1961. The thermohaline circulation in relation to the general circulation in the oceans. *Deep-Sea Res.* 8:39–64
Yang J, Neelin JD. 1993. Sea ice interactions with the thermohaline circulation. *Geophys. Res. Lett.* 20:217–20
Yasuda I. 1997. The origin of North Pacific Intermediate Water. *J. Geophys. Res.* 102:893–909
Yasuda I, Okuda K, Shimizu Y. 1996. Distribution and modification of North Pacific Intermediate Water in the Kuroshio-Oyashio interfrontal zone. *J. Phys. Oceanogr.* 26:448–65
Yin FL, Fung IY, Chu CK. 1992. Equilibrium response of ocean deep-water circulation to variations in Ekman pumping and deep-water sources. *J. Phys. Oceanogr.* 22:1129–57
Zhang RH, Levitus S. 1997. Structure and cycle of decadal variability of upper-ocean temperature in the North Pacific. *J. Clim.* 10:710–27
Zhang S, Greatbatch RJ, Lin CA. 1993. A reexamination of the polar halocline catastrophe and implications for coupled ocean-atmosphere modeling. *J. Phys. Oceanogr.* 23:287–99
Zhang Y, Wallace JM, Battisti DS. 1997. ENSO-like interdecadal variability: 1900-93. *J. Clim.* 10:1004–20
Zhang Y, Wallace JM, Iwasaka N. 1996. Is climate variability over the North Pacific a linear response to ENSO? *J. Clim.* 9:1468–78

Annual Review of Earth and Planetary Science
Volume 27, 1999

CONTENTS